ANALYSIS OF CRIMPING MECHANISM IN STUFFING BOX CRIMPER

BY

NORIYUKI KOUGUCHI

S.B., THE UNIVERSITY OF TOKYO

(1958)

SUBMITTED IN PARTIAL FULFILLMENT

OF THE REQUIREMENTS FOR THE

DEGREE OF MASTER OF

SCIENCE

AT THE

MASSACHUSETTS INSTITUTE OF

TECHNOLOGY

JUNE, 1966

SIGNATURE of AUTHOR.....

DEPARTMENT OF MECHANICAL ENGINEERING,

FIBERS AND POLYMERS DIVISION, MAY 17, 1966

CERTIFIED BY....

THESIS SUPERVISOR

ACCEPTED BY.....

CHAIRMAN, DEPARTMENTAL COMMITTEE

ON GRADUATE STUDENTS

ABSTRACT

ANALYSIS OF CRIMPING MECHANISM IN STUFFING BOX CRIMPER

by

NORIYUKI KOUGUCHI

Submitted to the Department of Mechanical Engineering on May 17, 1966 in Partial Fulfillment of the Requirement for the Degree of Master of Science.

In this thesis, the basic mechanism for the stuffing box crimper was investigated and made clear. The basic characteristic, the crimp length l_c, is determined by the geometry of the small crucial region, an immediate neighborhood of the nipping point of the feed rolls. The geometry is controlled by the numerous factors such as, yarn velocity V, bending rigidity of the fiber EI or ED which is strongly affected by temperature, stuffing box pressure P_s, radius of the roll R, width of the stuffing box W, friction coefficient μ, number of filament N, and nipping pressure P_n. Furthermore, since there are primary and secondary fluctuations in the geometry of the foundation, the actually resulted crimp length l_c is not regular but rather widely distributed.

Making the analyses carried out into a non-dimensional form,

$$\frac{l_c^2 P_s d^2}{"EI"} = A\,(W/R)^m\,(V\,d\mu/dV)^n\,P(R,EI,N,T,\mu)_1$$

More specifically,

$$\frac{l_c^2 p_s}{D} = 1.85\times10^{-11}\,(W/R)^{-1.75}\times \{0.18+0.78(V/V_o)-0.063(V/V_0)^2\}\times P(R,EI,N,T,\mu)$$

for Nylon 66 yarns, E and ρ of which are estimated as 1.0×10^5 Kg/mm^2 and 1.14 g/cm^3 respectedly.

Thesis Supervisor: Stanley Backer

Title: Professor of Mechanical Engineering

ACKNOWLEDGEMENTS

In carrying out this thesis work, I am deeply grateful for the valuable suggestions which grew out of the discussions with my thesis supervisor, Prof. Stanley Backer and also with Dr. Peter Popper. Furthermore, I would like to acknowledge the help and encouragement offered by my colleagues in the Fibers and Polymers Division.

I also express my deep gratitude to my wife, Kayoko and my son, Hiroyuki, who have sacrified a great deal so that I might have the opportunity to write this thesis. Their wonderful letters have helped me through difficult and depressing days.

TABLE OF CONTENTS

CHAPTER 1 Introduction

More than two decades have passed since "Nylon",the pioneer of the synthetic fiber and still predominant one, was introduced by Carothers in 1938. Du Pont's propaganda for promoting its sales was "the fiber, more slender than the thread of cob-web, stronger than steel, brighter than silk, and produced by air and water". But the essential features in comparison with so-called natural fibers are its endlessness and straightness with smooth circular cross section.

During the introductory period in which Nylon, Polyester, and Acrylic fibers were commercially produced, their producers had been expanding their sales mainly by taking advantages of these essential characteristics, in other words, those which the natural fibers do not have. For example, slenderness and high strength led to the huge consumption of Nylon stockings and low moisture content and high bending rigidity threatened the cotton industry with the catch-phrase "Wash and Wear". However, these characteristics did not satisfy the human desire for softness, bulkiness, or high moisture absorption which the natural fibers, wool and cotton, have to a great extent. These demands motivated the producers to develop modification techniques which often led to a compromise, i.e., blending with natural fibers. In the process of staple fiber production, it has been quite common, or more strictly speaking, indispensable to give a crimped shape or waviness to the

fiber in order to provide fiber assembly cohesion to permit handling. This idea, naturally gained by the study of the natural fiber's shape[1] and furthermore stimulated by the demand toward softness and bulkiness of the fabrics, has resulted in the processes of manufacturing "textured yarns".

Historically the process for texturizing yarn was first seen toward the end of the last century when there was no man-made fibers. The most primitive and still widely used devise is "stuffing box method". It consisted of the axially-split cylinder with many small holes.[2] The cylinder was held together in advance by bolts and nuts, and hemp, lincoln wool or sometimes cotton were stuffed into it by means of man power , hydraulic power or etc.. The gases which were generated by compression or heating of the stuffed materials escaped through the holes. The processed materials in this way then was heated up from the wall of the cylinder or directly in the hot water bath for setting. In contrast with the above-mentioned batch-method, the continuous type[3] appeared around the same time. It consisted of a pair of feeding rolls and a stuffing box where yarns fed in received compression for a while. Although the stuffer element sometimes was realized in the form of a pair of belt-conveyers,[4] these two basic elements, the feed roll and the stuffing box, have remained essentially unchanged up to the present time.

The present day texturizing method was initiated by

Alexander Smith and Sons[5], a leading carpet manufacturer. In 1948[6] Smith was investigating the reason for the great superiority of Indian wool, costing about $.42 per pound, over South American wool, at $.18 per pound. Research teams investigating the two types of wool determined that chemically they were identical but came to the unexpected conclusion that the main difference was in the crimp of the Indian fiber versus the South American wool, which was almost straight. Workers were able to prove that the difference in properties between crimped and uncrimped wool was greater than the difference between wool and cotton. By 1950, Alexander Smith designed a commercial machine to crimp South American wool fibers and saved a substantial amount of money by doing so.

In 1951, Joseph Bancroft[7], an outfit specializing in developing and licesing fabric finishes, purchased the license for this invention and applied it to Nylon filament yarns. The new yarn had improved its resilience, much greater abrasion resistance, warmth due to the air retained among the crimped fibers, and comfort in wear. Texturized synthetic yarns now had a widened application due to the Bancroft process togetherwith several other techniques developed for the purpose, which will be summarized in the next section. These application included socks, sportswear, children's wear, men's suiting, underwear, gloves,and etc..

1-1. Texturizing Methods

In this section a brief review of various methods for manufacturing "textured yarns" is presented for reference purposes. There exist several ways of classification, but generally they may be classified as shown in Table 1.

1. Conventional method: Scheme is shown in FIG 1. First twisting up to 50-90 T/inch, then heat setting at 110-130°C for about 60 min, thereafter untwisting to almost 0 twist, then a little retwisting to reach no- torque condition.

2. False-twist method: Scheme is shown in FIG 2. False twist spindle of high revolution gives twisting and untwisting continuously to the yarn. In front of, sometimes also at the rear of, False-twist spindle there are heat setting zones respectively.

3. Edge-crimping method: FIG 3 shows its schematic view. Passing around the knife-edge the outside portion of the yarn is stretched, whereas the inner one is compressed togetherwith the generation of heat. Hence the former becomes more oriented, the latter reduces its degree of orientation. These two different molecular structures, after fixed, deform the yarn into a spiral configuration.

4. Stuffing box method: This will be detailed later

5. Air-jet or Steam-jet method: Scheme is shown in FIG4. Air or steam-jet with high speed impinges on the yarn turbulently, which is overfed into the nozzle slantwise with the

Table] Texturizing Methods[8)]

Method	Application	
	Continuous filament	Staple fiber
] conventional(multi-staged twisting) method	x	
2 False-twist method	x	
3 Edge crimping method	x	
4 Stuffing box method	x	x
5 Air-jet or Steam-jet method	x	
6 Gear crimping method	x	x
7 Chemical treating method	x	x
8 Conjugated (Bi-component) method	x	x
9 Knit-heatset-unravel method	x	x

direction of the nozzle axis, therefore the yarn becomes interlaced and bulky. Steam-jet improves its bulkiness due to the additive effects of heat and moisture.

6. Gear crimping method: FIG 5 shows its schematic view. Heavily crimped yarns result by crimping passing through a pair of geared wheels which are usually warmed up.

7. Chemical treating method: This method was developed sometime ago in the process of manufacturing Rayon staple yarn. It is an application of the difference of the contraction behavior between sheath and core which results from the coagulation process in the so-called spinning bath. Recently a method which seems to belong to this category has been developed for Nylon [9]. This method consists in a combination of chemical treatment by phenol and physical treatment by supersonic wave apparatus.

8. Conjugated(bi-component) method: Early studies of the wool configuration and of crimped Rayon staple yarn [1] showed a bilateral structure and a sheath and core structure respectively. This idea was first introduced by Sisson [10] in his patents earlier for Rayon, but it had not drawn much attention until du Pont submitted its technique applied for synthetic fibers in 1955, and put these fibers into market under the names of Orlon Sayelle Type 21, 24, and 27 [11]. The basic idea consists of the simultaneous spinning of the two different polymers. Although the essential technique for this

method lies in the designing of complicated spinning nozzle apparatus and the good combination of two adequetly different polymers, the priciple is fairly simple and its mechanics has been investigated by Brand and Backer[12].

9. Knit-heatset-unravel method: This is very primitive but still used sometimes. The idea is to take advatage of the configuration of warp or filling yarn in the fabrics.

In Table 2 we show the characteristics of the yarns produced according to the above-mentioned methods presumably at conventional speed[13].

1-2. Purpose of this Analysis

Among the various methods of texturizing briefly reviewed in the previous section, the method of "stuffing box type crimping" is one of the most popularly adopted technique due to the following reasons;

1) Simple mechanics, in principle consisting of a pair of feed rolls and a stuffing box where the yarn is compressed for a while.

2) High productivity, partly due to its simple mechnics, largely due to its seemingly simple mechanism, which results in the only one mechanical technique in case of staple fibers except the gear crimping method.

3) Unique configuration, i.e. zig-zagged waviness, giving an effect of tassel-like feeling.

4) Non-torque yarn but rather three dimensional crimp,

As a consequence, this crimped yarns are utilized in the various fields, under the trade-names of "Banlon", "Perlon-Nevaflor", and etc. But on the other hand this simple mechanism of crimping yields a few disadvantages to the other methods, such as a large dustribution of waviness and various temparature effects. For overcoming these advantages many investigations have been taken every year, judging from the number of the patent application. Of course those texts of patent sometimes indicate a kind of implication of what the most important factor is in this mechanism, nevertheless, there have been few published reports about this seemingly simple mechanism.[4) 5)]

In this thesis, the auther intends to investigate in great detail the actual phenomena of buckling in the crucial small region where the crimp mechanism initiates. From observations on monofilament and sometimes multifilament togetherwith experimental crimp results, we hope to find a relationships between the final crimp configuration and the various properties of the material, or the environmental conditions. From analysis of such experiments it should also be possible to obtain a good insight into the effect of crimp during the processing of staple fibers.

Table 2

Mehtod	Characteristics of yarns	production speed
] Conventional	fairly uniform, good crimp, highly elastic, alittle stiff feeling	ft/min ~5
2 False-twist	uniform, lower elasticity, good feeling, high bulkiness	~50
3 Edge crimping	non-torque, high bulkiness, higher elasticity, good stability, uniform	]00-300
4 Stuffing box	irregular, zig-zag waviness, soft feeling, low elasticity	-]500 -200*
5 air-jet	similar to those of methd.], less uniform, low pilling resistance	]50-400
6 Gear crimp	regular waviness,	-]800
7 Chemical	low elasticity, good feeling	-]50 ?
8 Conjugated	three-dimensional crimp, low elasticity, uniform, good feeling	-]500 ? spinning speed
9 Knit unravel	large crimp, uniform,	?

* for staple yarn

CHAPTER 2 Experiment

2-1. Experimentation

The general views of the experimental device are shown in FIG. 6 and FIG.7, the latter showing the general assembly togetherwith the yarn packages.

The schematic diagram of the general arrangement is shown in FIG.8, in which 1 are yarn packages from which the unwound yarn goes through the disc-type tension device 2 and is fed into the nipping point of a pair of rolls 4, one of which is positively driven and the other an idler roll which presses against the other roll with a spring force 5 which can be adjusted by a screw. The yarn seperating guide 3 is inserted between 2 and 4. The yarn thus fed is accumulated in the stuffing box 6 under the pressure by means of the dead weight 7. The sideplates of the stuffing box are made of the transparent "Plexyglass" so that the crimping phenomena could be looked in. The D-C motor of 1/15HP 9 with the Variac speed control 10 controls the speed of a roll through the chain-sprocket speed reducer 8. The more detailed sketch FIC9 shows the face-view of the main device and FIG.10 does the side-view.

1. A pair of rolls, two different sized rolls, 2 and 3 inch diameter with 1/2 inch thickness fixed, are available, miller finished surface of stainless steel.

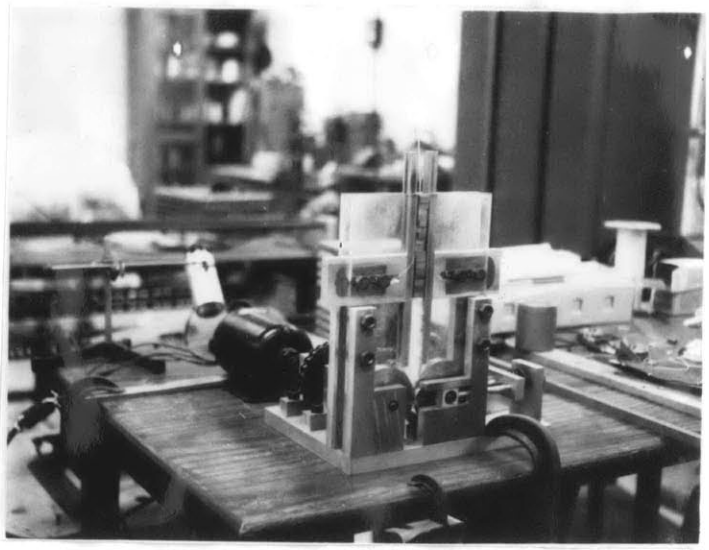

FIG.6 GENERAL VIEW

FIG.7 GENERAL VIEW

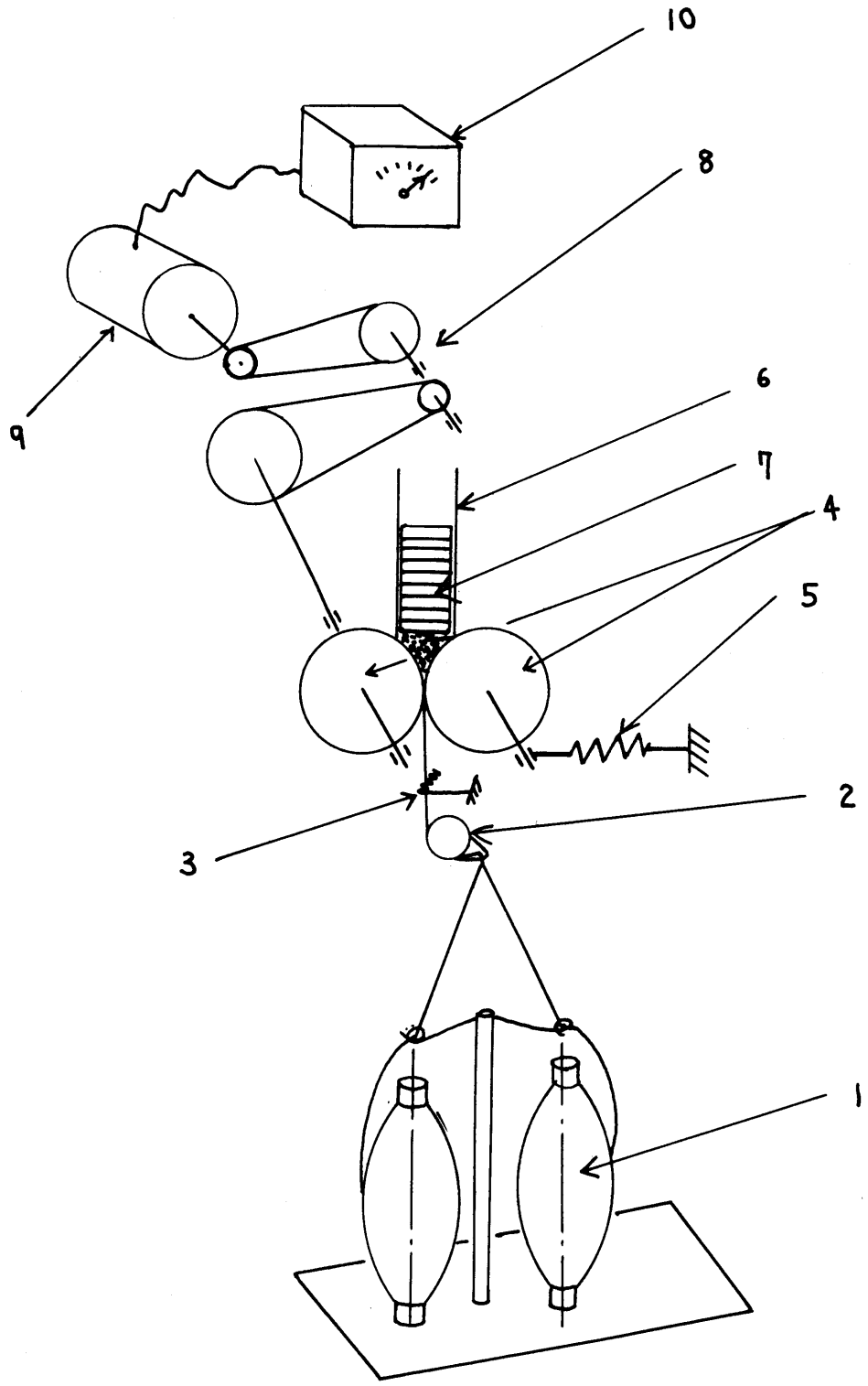

FIG.8 GENERAL ARRANGEMENT

2. Sliding plates, the distance of the plates, called W, can be adjusted by the holder 7. The tips are made of Teflon to avoid abrasion.

3. Side plates, made of Plexyglass

4. Housing

5. Pushing bar, which presses the idler roll against the positively driven roll by means of spring, the force of which can be varied by screw 6.

The special arrangement for looking at the crucial region of crimping is schematically shown in FIG. 11. 1 is the positively driven roll, 2 is made of transparent material and deeply recessed-in which enables us to see the crucial region 4 through the reflecting miller 3.

2-2. Experiment

2-2-1. Preliminary Experiment

To grasp a crude idea of crimping mechanism at first, preliminary experiments were run by using 380 denier Nylon 66 monofilament. Because of its extraordinarily high bending rigidity in comparison with that of the actually processed fine denier yarns, even the crucial region could be observed through a telescope.

The building-up of foundation, which means the fiber assembly of the crimped yarn under pressure and is so called henceforth, is shown by FIG. 12 and the resulted crimped yarns are shown in FIG 13.

The results obtained here are;

]) Crimping mechanism is actually a twist bending in the tiny region between the nipping point and the tip of the foundation. The twisting which is clearly shown in FIG.]3 is caused by the flattening of the originally circular cross section due to the nipping pressure, because the minimum strain energy priciple requires the bending in the direction of the lower bending rigidity and the twisting energy is usually far smaller than that of bending.

2) From the photographs of FIG.]2 building up mechanism of the foundation is not steady but first fluctuate alternatively in the direction of the axis of roll in the vicinity of the tip (which is defined "primary fluctuation) and secondly and macroscopicly fluctuates in the direction perpendicular to the axis of roll in the delta region.

3) Since there is a twisting, the resulted crimp yarn is in three dimensional configuration as shown in the top picture of FIG.]3.

4) The middle pictures show that the crimp waviness is quite dependent of the geometry of the device, since those two different crimpnesses were resulted by just changing the roll radius R.

2-2-2. Experimental Results

2-2-2-]. Definition

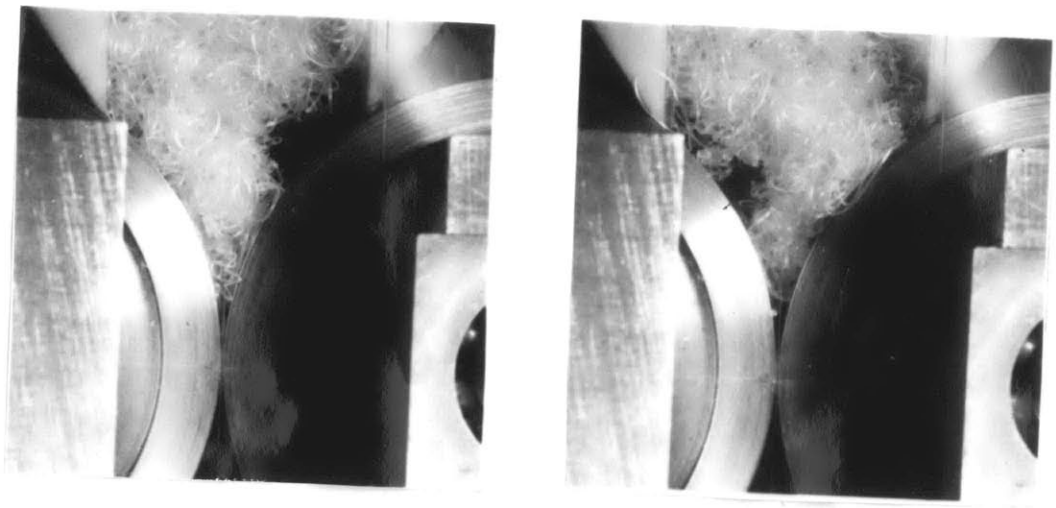

2 INCH ROLL

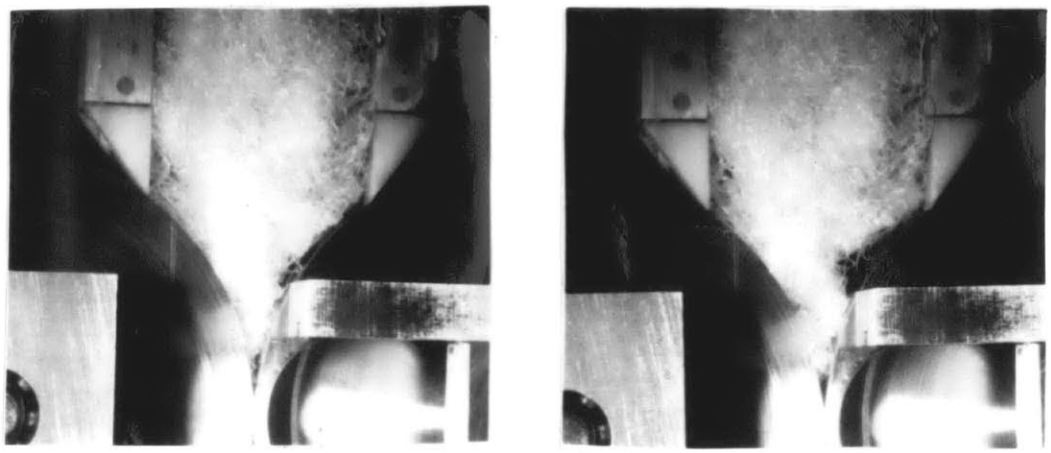

3 INCH ROLL

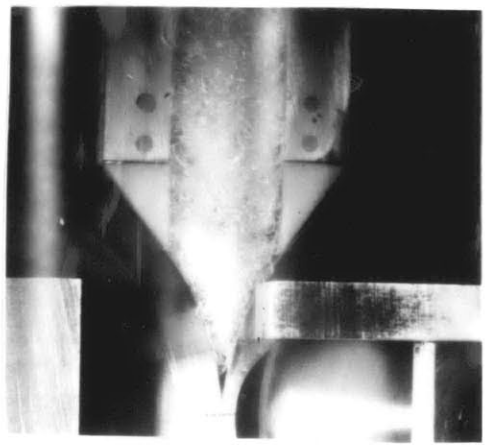

380 DENIER NYLON 66

FIG. 12 BUILD-UP OF FOUNDATION

Although there are several ways of describing the crimp characteristics, the two basic parameters for the fundamental investigation are defined as follows (see FIG.14),

Crimp Length (l_c)

Crimp Angle (θ_c)

From the above definitions, the two commonly used parameters Crimp frequency C_f, Number of crimps C_n per extended fiber length L_o and Crimp index C_i, the extendable length d of a crimped fiber devided by L_o are represented as follws,

$$C_f = C_n / L_o = 1/ 2l_c$$

$$C_i = d/ L_o \times 100\% = (2l_c - 2l_c \sin\theta_c)/ 2l_c \times 100\% = (1-\sin\theta_c) \times 100\%$$

2-2-2-2. Qualitative relations among the various factors

From the previous preliminary experiment, the following qualitative relationships can be established among the properties of materials, the dimensions of the geometry and the other environmental conditions.

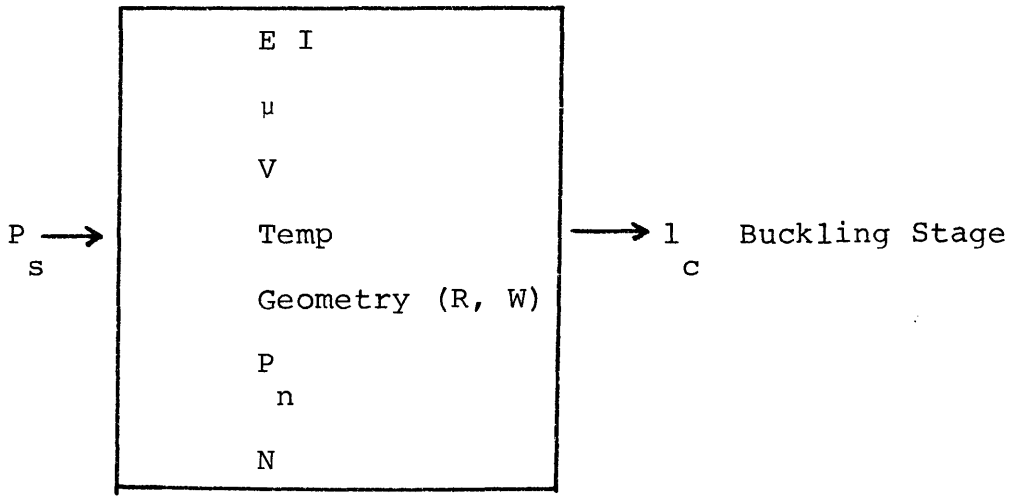

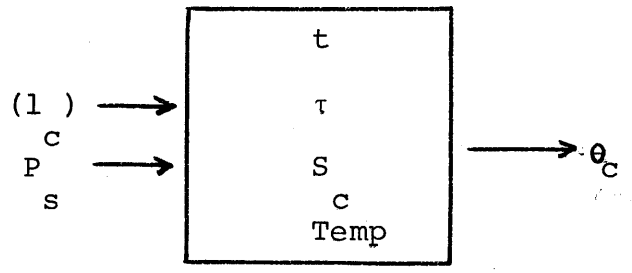

Setting Stage

1) Buckling Stage

In this stage, crimp length l_c is determined. Among the various factors P_s (stuffing box pressure), EI (bending rigidity), μ (friction coefficient), P_n (nipping pressure affecting the effective bending rigidity "EI"), N (number of filaments also affecting "EI"), and Temp (temperature affecting Young Modulus E) are the factors determining the characteristics of the foundation. R(radius of roll), W(width of the stuffing box), yarn speed V and μ are the determining factors of the geometry of the foundation. To emphasize the common importance of P_s in the commercial production P_s is put outside of the box.

2) Setting Stage

In this stage, the yarn,which was fairly completely buckled into the folded configuration,will recover under the pressure in the foundation as shown in FIG.15. This recovery behavior and setting process are controlled by processing time **t**,relaxation time τ, and crystalization speed S_c. The latter two factors are influenced to a great extent by temperature Temp. Temperature effect for the relaxation time τ is replaced by **t** because of the

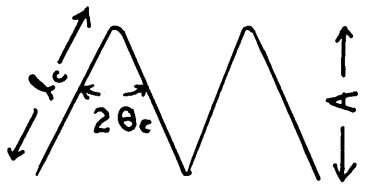

FIG.14 DEFINITION

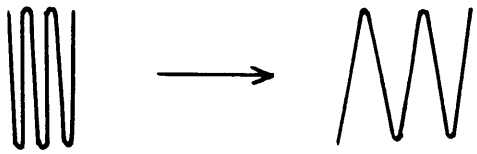

FIG. 15 RECOVERY OF CRIMPED YARN

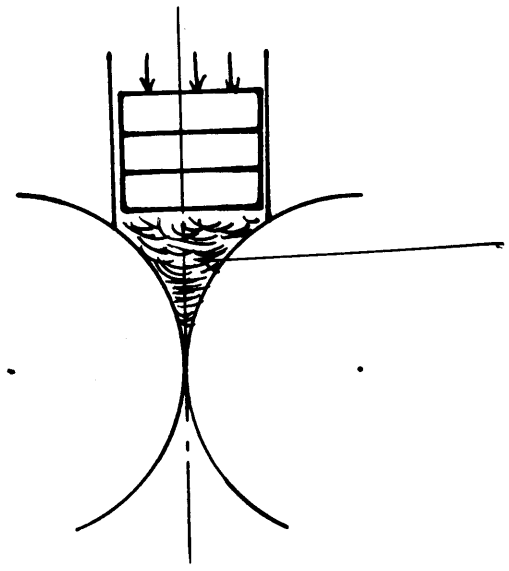

DELTA REGION OF FOUNDATION

FIG. 16

Temp-time superposition principle and τ is generally decreased as temperature increases. But S_c has generally a peak at certain temperature, therefore there is some optimum temperature for a suitable setting condition. Since the principal purpose of this thesis is to investigate the basic phenomena and their mechanism and the setting condition or mechanism have been fairly well researched, all the experimenrs are concerned with the buckling stage.

2-2-2-3 Design of Experiment

To get efficiently the various relationships among the many factors, the following scheme of experiment was designed as shown in Table 3.

The experimental conditions are;

Yarn speed: V

V_{11}	35.6 ft/min	for R_1 roll
V_{12}	83.4	
V_{13}	131	
V_{14}	260	
V_{21}	53.4	for R_2 roll
V_{22}	125	
V_{23}	197	

Yarn denier: D

D_1 7 denier- 1 fil.

D_2 15 - 1

D_3 30 - 1

D_m 70 - 34

Pressure: P_s

P_{s11}	116.7	g/in^2	for W_1
P_{s12}	233.4		
P_{s13}	406.0		
P_{s21}	124.5		for W_2
P_{s22}	249.0		
P_{s23}	410.5		

Width: W

W_1 9/16 inch

W_2 13/16

Clearance between W and dead weight is 1/16inch.

Number of Filaments: N

N_1 1

N_2 2 spacing is 1/16 inch

n_3 3

N_m 34 1/2 Z twist

Diameter of Roll: R

R_1 2 inch

R_2 3

Process time; t

t_1 10 min

This time is measured after the steady state is reached, which means the state where the fiber assembly fills up the top delta region of the foundation as shown in FIG.16.

Nipping pressure: P_n

P_{n1} 10 lb/in

P_{n2} 25

P_{n3} 40

Material: du Pont's Nylon 66, Type 280 Semidull, the strain-stress curves are shown in FIG.17.

Room Condition:

Temperature 67° F

Humidity 60 %

2-2-2-4 Experimental Results

2-2-2-4-1 Relationships

After ten minutes passed, the dead weights are taken out and then crimped yarns are slowly pulled out. After the inked mark which shows that the yarn is processed in the steady state was pulled out, several portions of the yarn was cut out in length of about 2-3 inches by a scissor at random and the four of them are laid between the micro slides under a small tension which makes the measurement under microscope easier. Through the microscope

the crimp length l_c is measured at ten different positions at random. After making an average X_{10}, then five quantities near to the X_{10} are again averaged. Then this X_5 is converted to an actual l_c in millimeters. These results are shown in Table 4 to Table11 and FIG.18 to FIG.25.

2-2-2-4-2. Observation of Buckling Region and Primary Fluctuation of Foundation

The observation was made with help of the special device indicated in FIG. 11 and the intermittent sketches are shown in FIG.26 and their schematic view of the buckling history in FIG.27.

2-2-2-4-3. Simulation of Buckling Region

Using a thin copper wire which is almost plastic, a simulating experiment was carried out and the result is shown in FIG.28. FIG.29 shows the schematic view, in which 1 and 2 are transparent plates having a small hole respectively through which the thin wire 3 is pushed in by a steel wire pusher 5 through a supporting cylinder.

2-2-2-4-4. Building-up of Foundation, Secondary Fluctuation

FIG.30, the corresponding schematic view in FIG.31 and so forth upto FIG.34 and FIG.35, show the history of the successive groups of the crimped yarn by intermittently inking the fed yarn at the tension device.

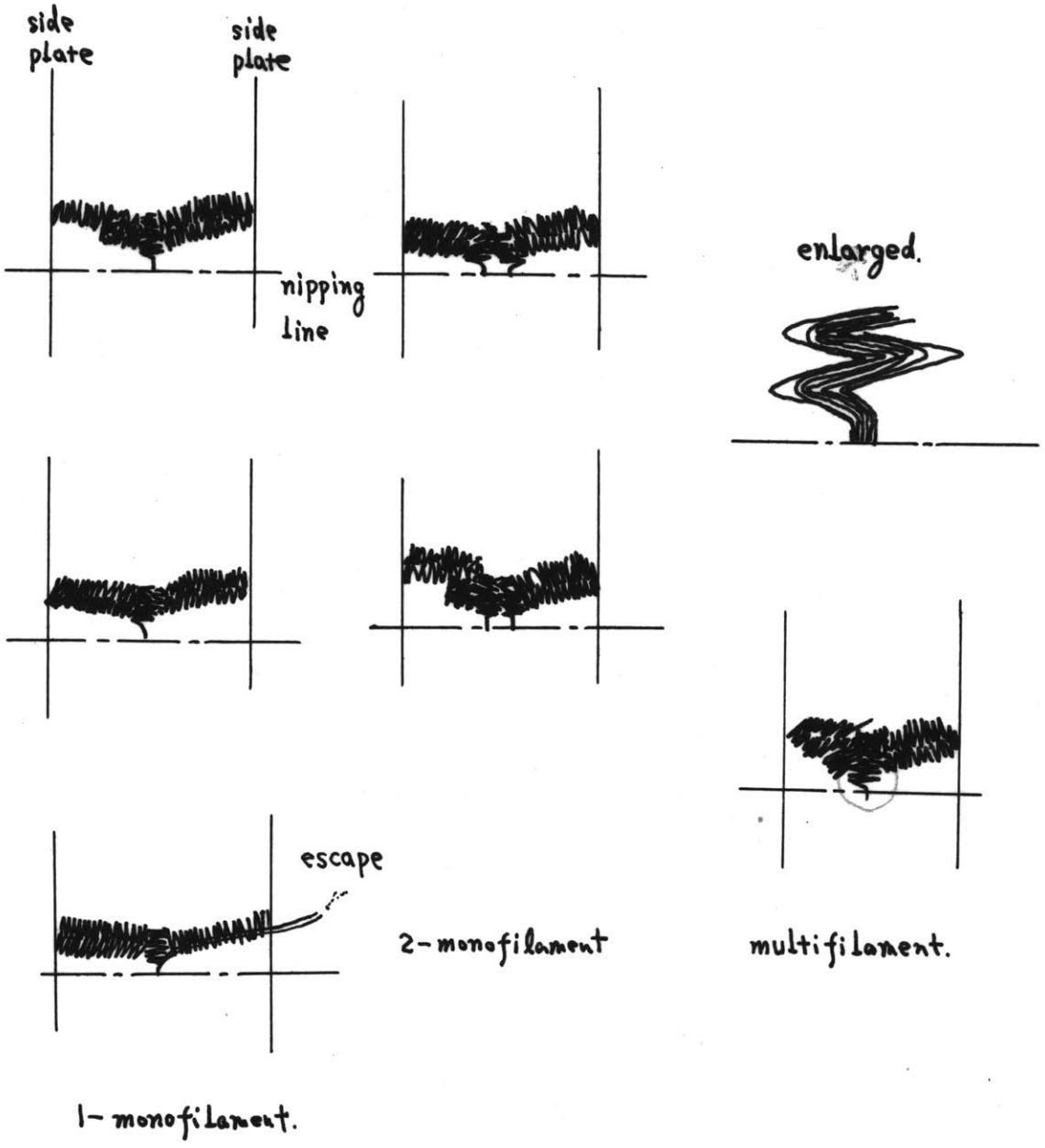

FIG. 26 SKETCHES OF BUCKLING REGION

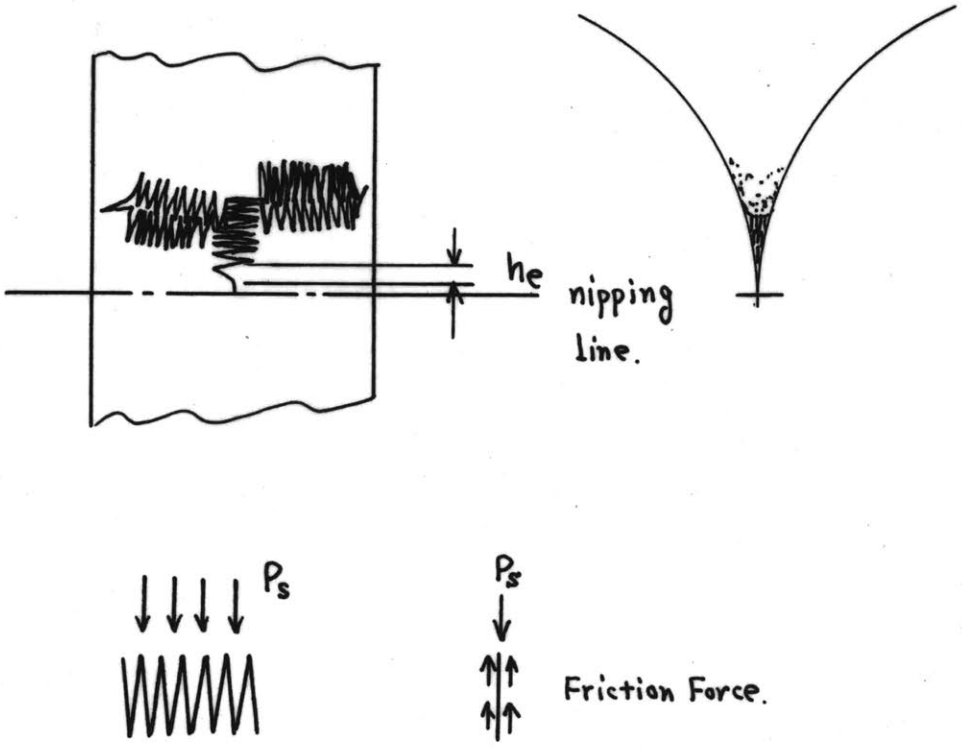

FIG. 27 Buckling History

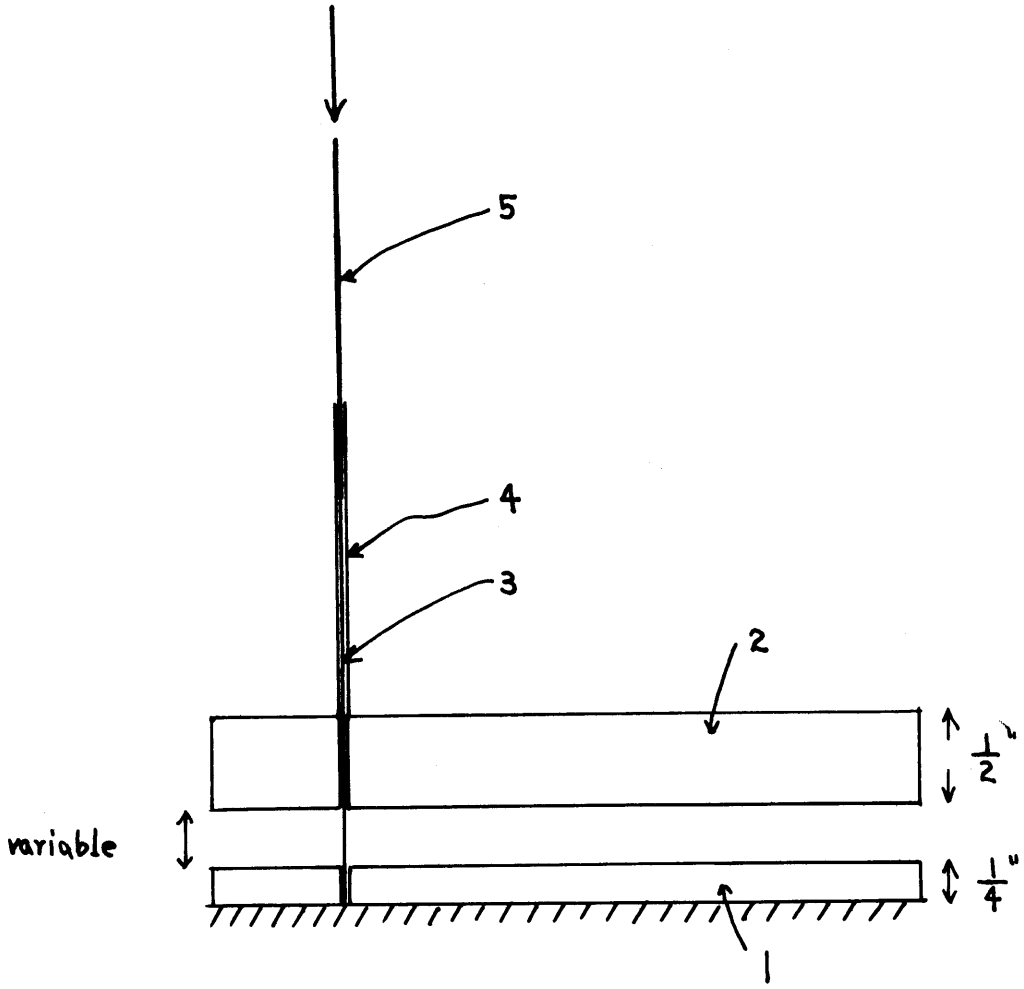

FIG.29 SCHEMATIC VIEW OF EXPERIMENT

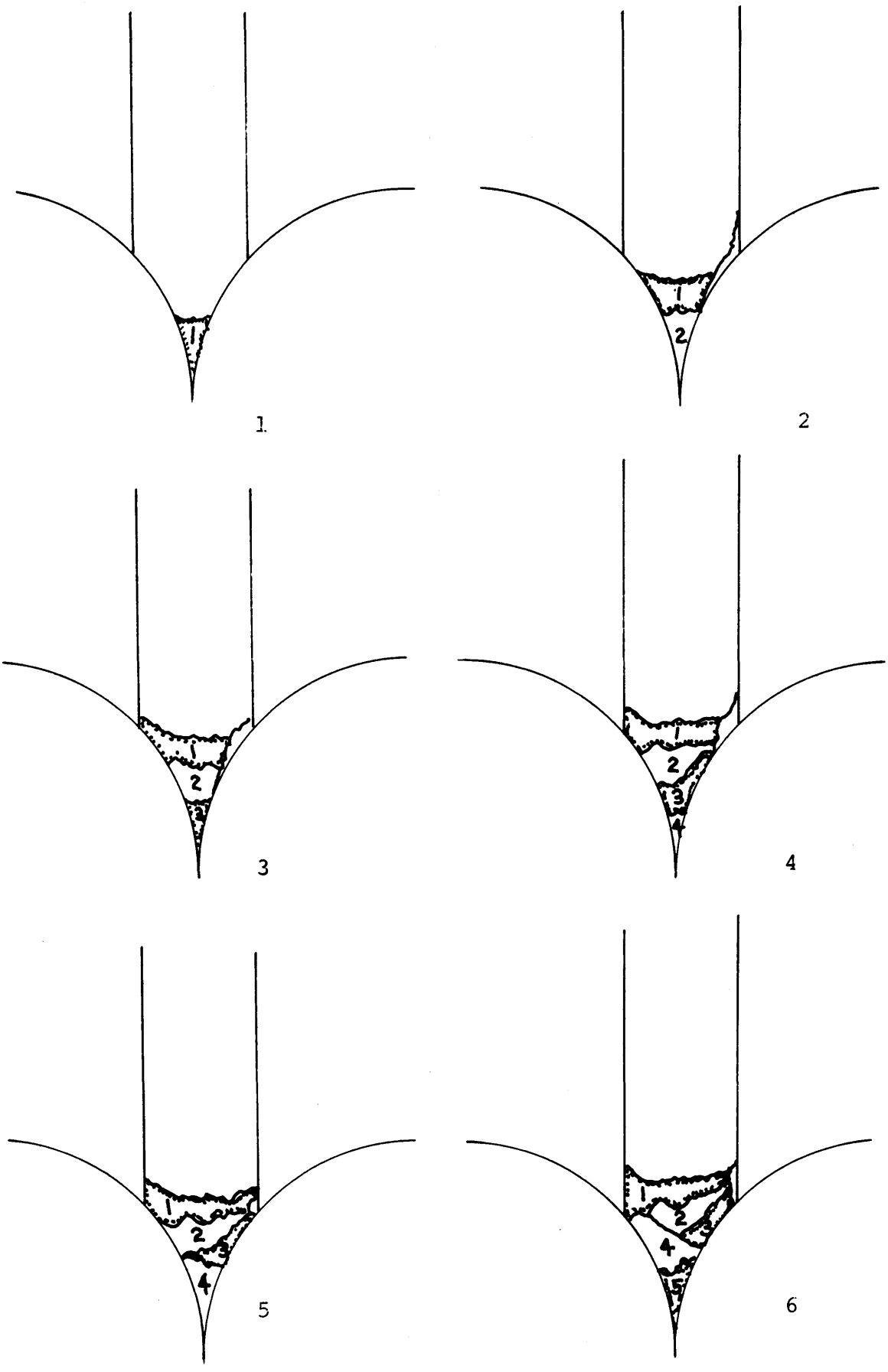

FIG. 31

7

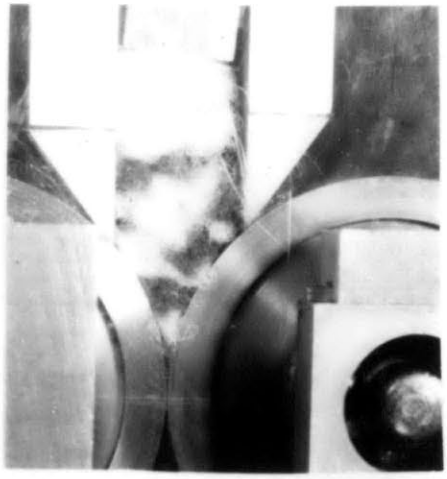

8

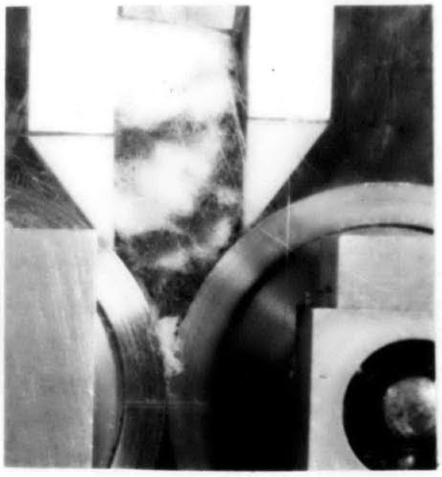

9

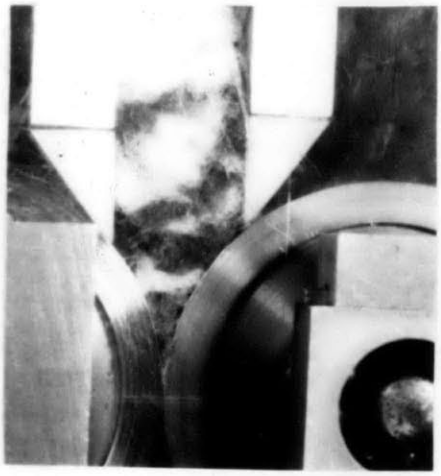

10

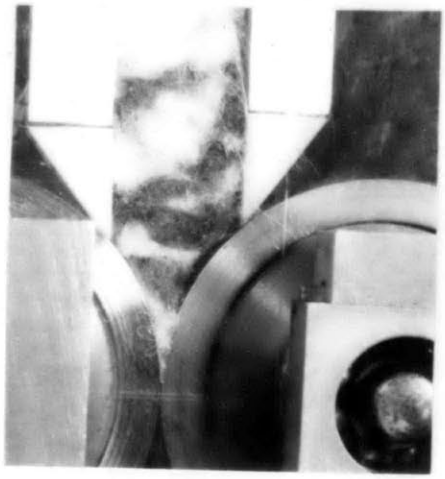

11

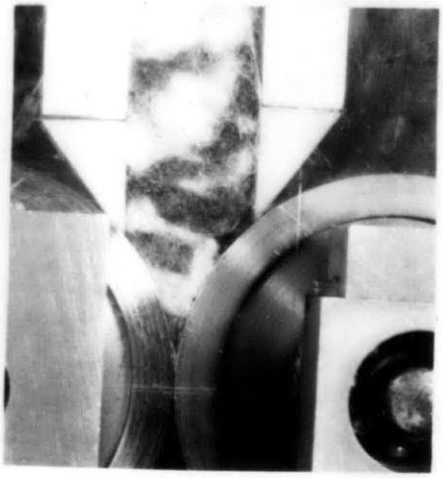

12

FIG. 32

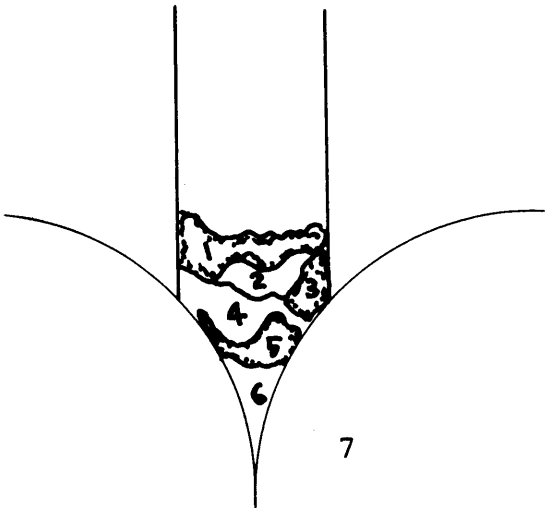

7

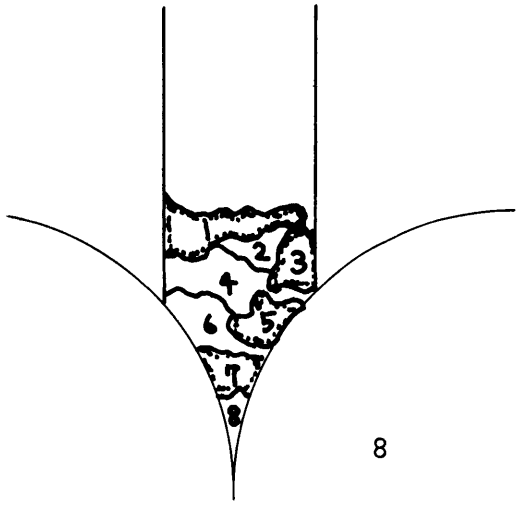

8

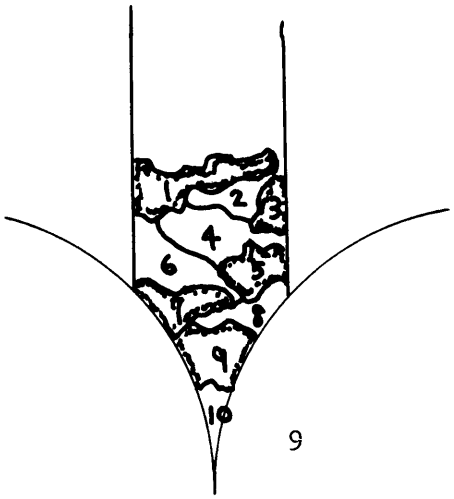

9

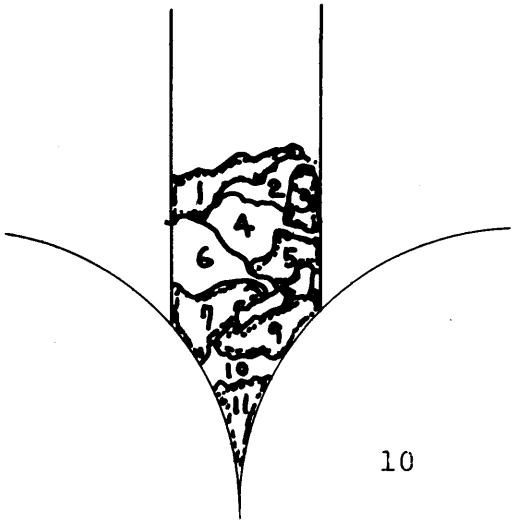

10

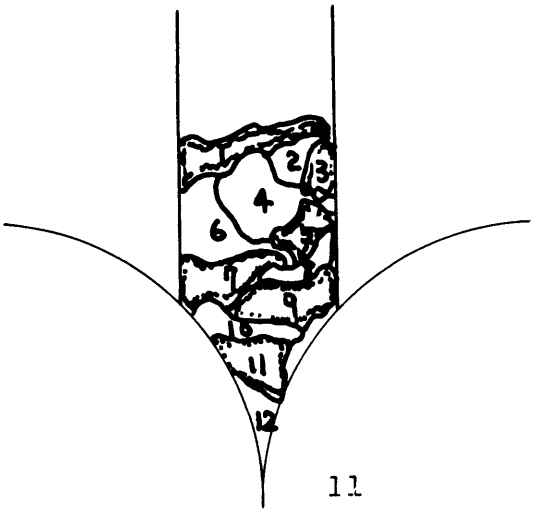

11

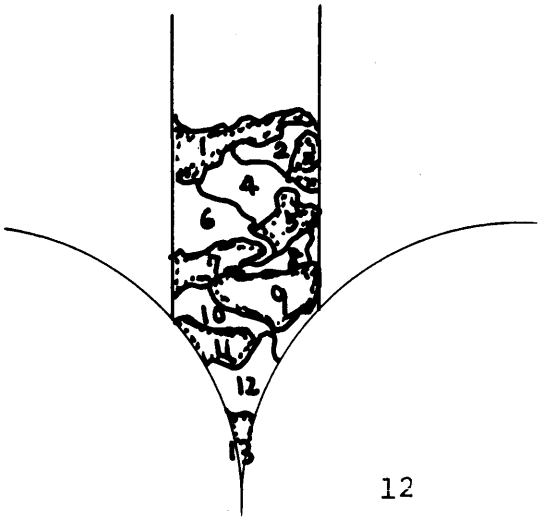

12

FIG. 33

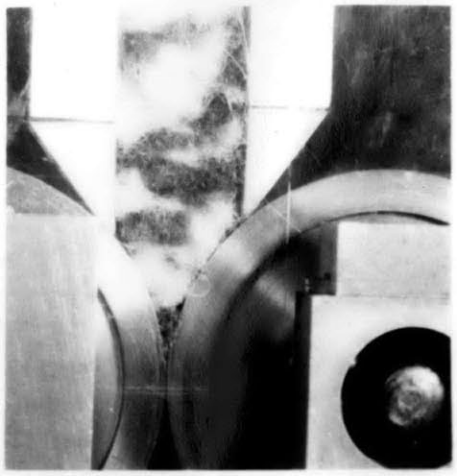

13

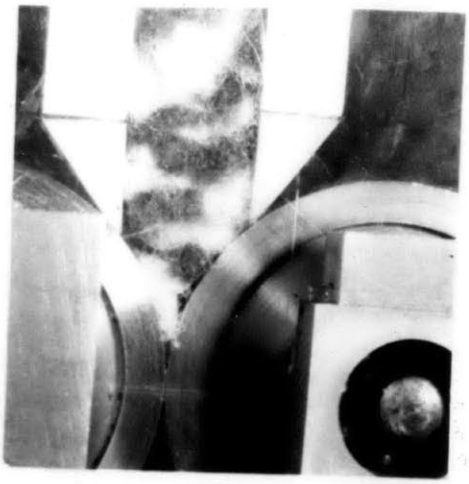

14

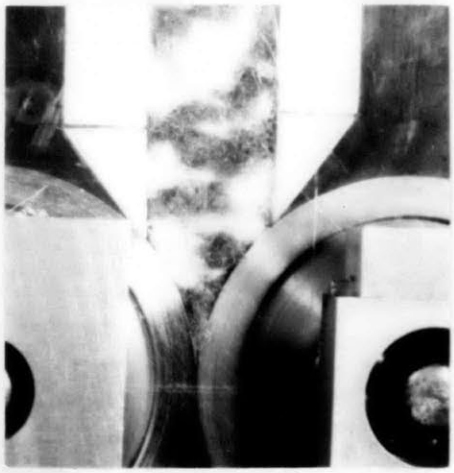

15

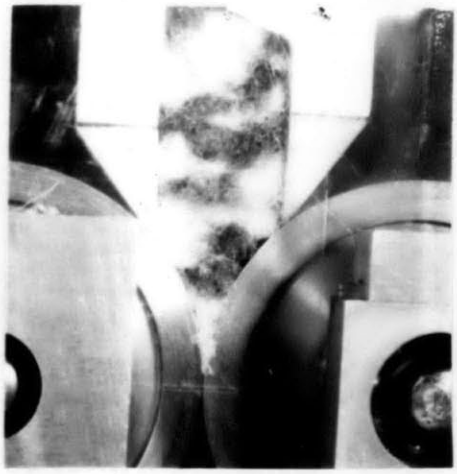

16

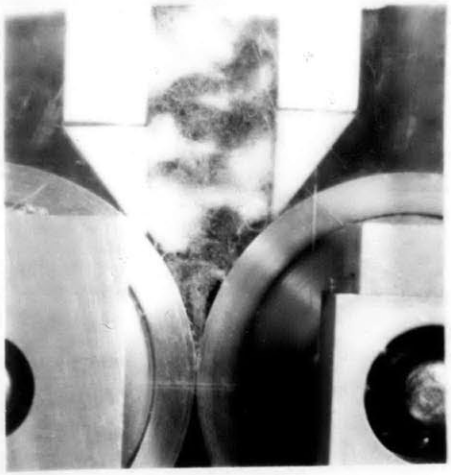

17

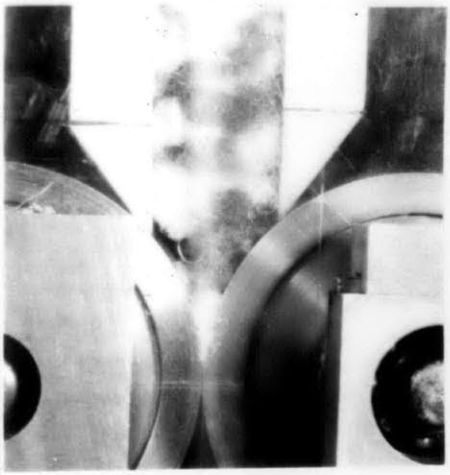

18

FIG. 34

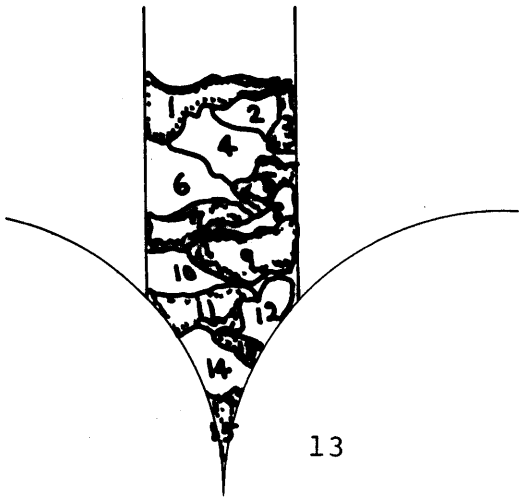

13

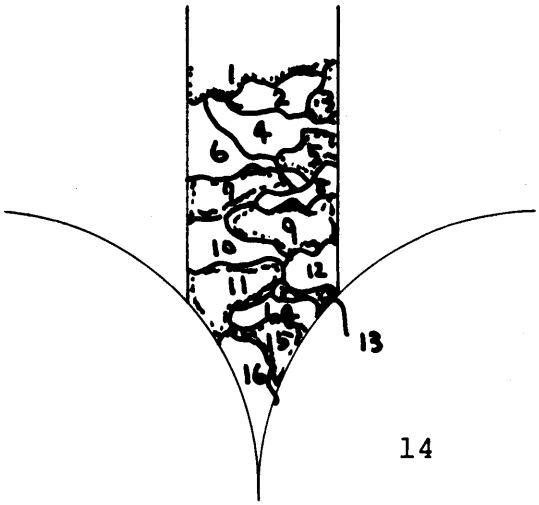

14

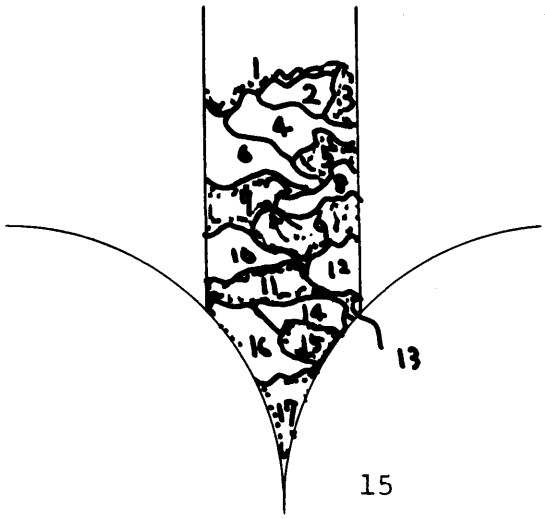

15

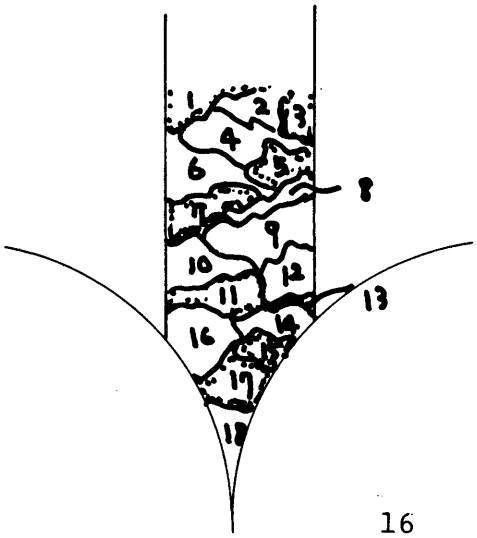

16

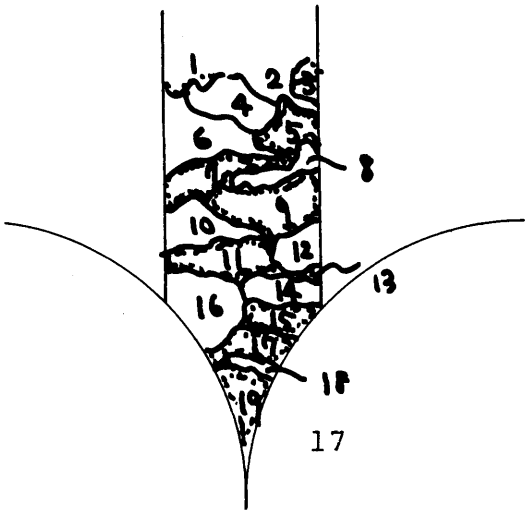

17

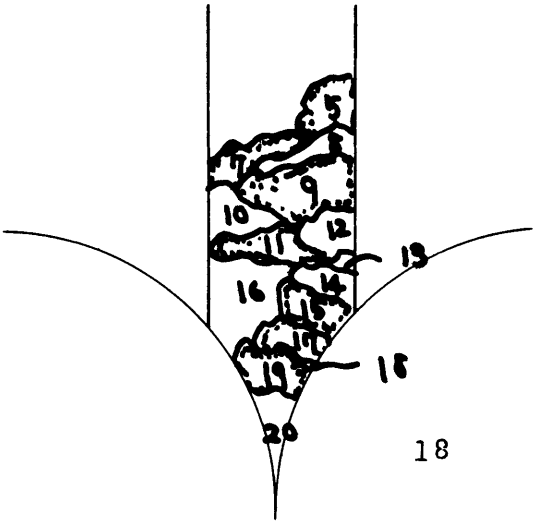

18

FIG. 35

The white portion and inked one have the same area approximately. The experimental conditions are:

V_{l1}	D 2	P_{s12}	W 1	R 1	N 2	P_{n2}

2-2-2-5. Summary of Experimental Results

1) General relationships among factors are briefly summarized in FIG.36.

2) Buckling mechanism is determined by the geometry of the crucial region.

3) Primary fluctuation is the main cause of the wide distribution of the crimp length l_c.

4) Effect of the nipping pressure is the higher probability for flattening of the round cross section in the case of mono-filament and negligible in the case of multi-filament.

5) Effect of the number of the filament seems to smooth out the irregularity of the primary fluctuation.

CHAPTER 3 Analysis

The careful observations described in the previous chapter have indicated that the crimping mechanism is a simple buckling one so that once the effective column height h_e is determined by the environmental conditions the crimp length l_c is fixed. Nevertheless, becuase of the fluctuation of the geometry in the crucial region the actual crimp length l_c is not regular but widely distributed.

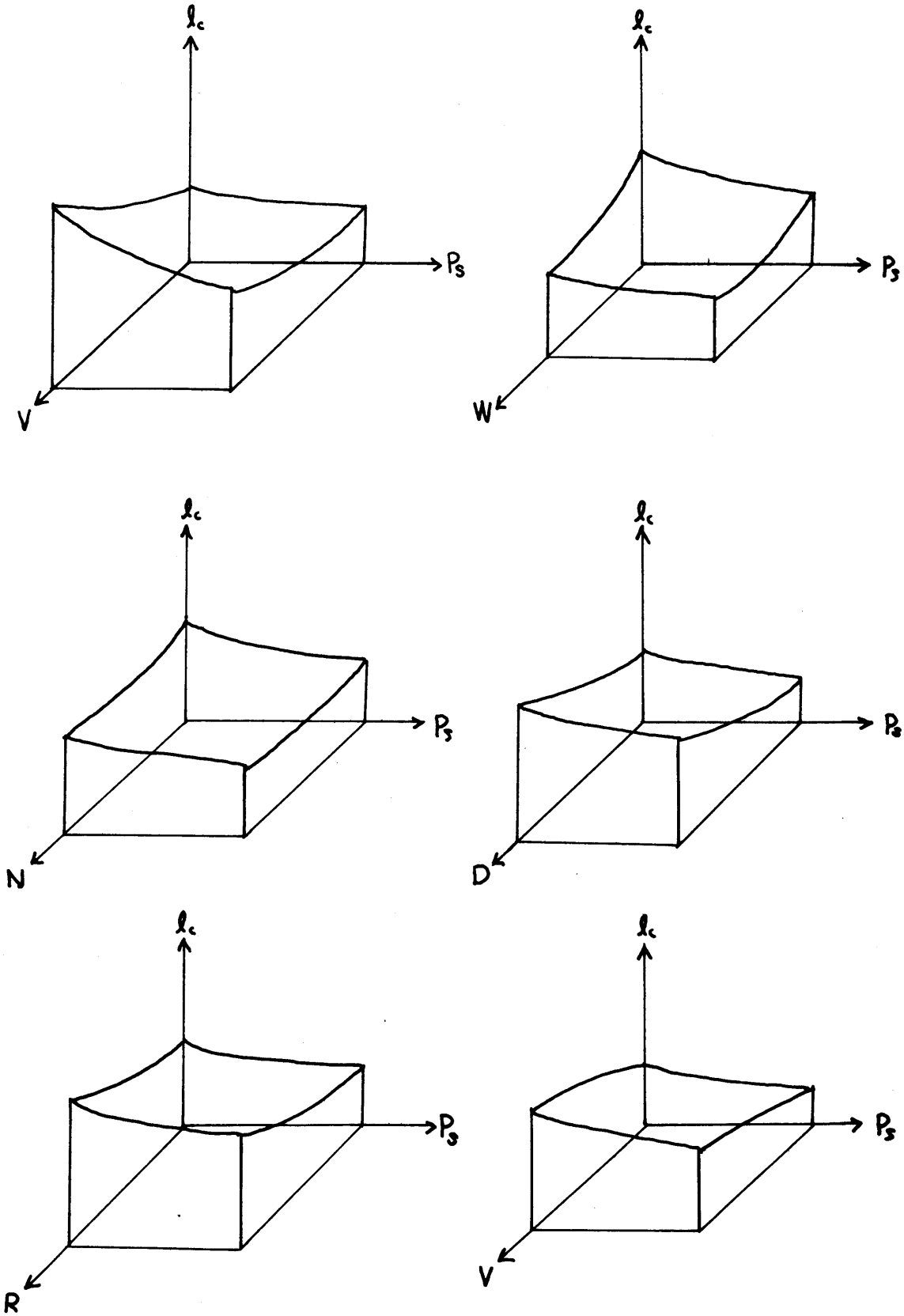

FIG,36 SUMMARY OF EXPERIMENTAL RESULT

Since the whole process of the stuffing box crimper can be devided into three stages; (buckling stage, the formation of foundation, and the determination of crimp angle θ_c), this chapter is arranged in that way.

3-1. Qualitative Analysis

3-1-1 Buckling Stage

Referring to FIG.26, 27, and FIG.28, when the effective column height h_e is once determined somehow the actual buckling mechanism can be modeled as shown in the successive diagrams of FIG.37. In case of mono-filament, since there is a little twist due to the flattening effect of the cross section the buckling plane is three dimensional. From the facts that when the running roll is suddenly stopped and the yarn just buckled is pulled out immediately from the crucial region the crimp disappears almost completely and that the material shows much higher Young Modulus in the rapid deformation, this buckling could be treated in the elastic region. Hence due to the end moment M in No.5 of FIG.37, the successive buckling takes place in the other half plane in stead of the same half plane as indicated in No.5' figure. The actual crimp length l_c is essentially determined by the effective height h_e as $l_c = h_e$, but the effect of the speed V should be considered here. By modeling it as in FIG.38, that is, the inertia force ρV^2 acts like the distributed axial force, the following equation

is given by Timoshenko[16],

$$h_e = \sqrt{m}\sqrt{\frac{EI}{P}} \tag{1}$$

where m is a function of $n = \rho V^2 h_e / \frac{\pi^2 EI}{h_e^2}$ (2)

the values of m are tabulated. Since P is the source of the strain energy of this system and the system will buckle in such a way that the strain energy should be minimum, it is reasonable to assume P is constant in the equation (1). Then m is a measure of h_e in some sense. The result is shown in FIG.39 and shows that there is essentially no effect on h_e by velocity V.

The configuration of the crimped yarn just before being compressed plastically by the foundation is not significant for the characteristics of the crimped yarns, but it could be solved in the following way. In general the model is like the one shown in FIG.40, where P_{sp} is a spring force and f_f is a frictional force, both of which result from the neighboring yarns, and f_i is an inertia force. If we are really concerned with the crimping of the staple fibers, the frictional force f_f could become significant. Symplifying this so complicated system, FIG.41 shows the case where the built-in column, the height l_c, is under P_s, M_t, M_b, and distributed force f_e which is equivalent to a combination of f_f and f_i. Furthermore if the buckling is assumed in the plane, the effect of M_t can be dropped. Then,

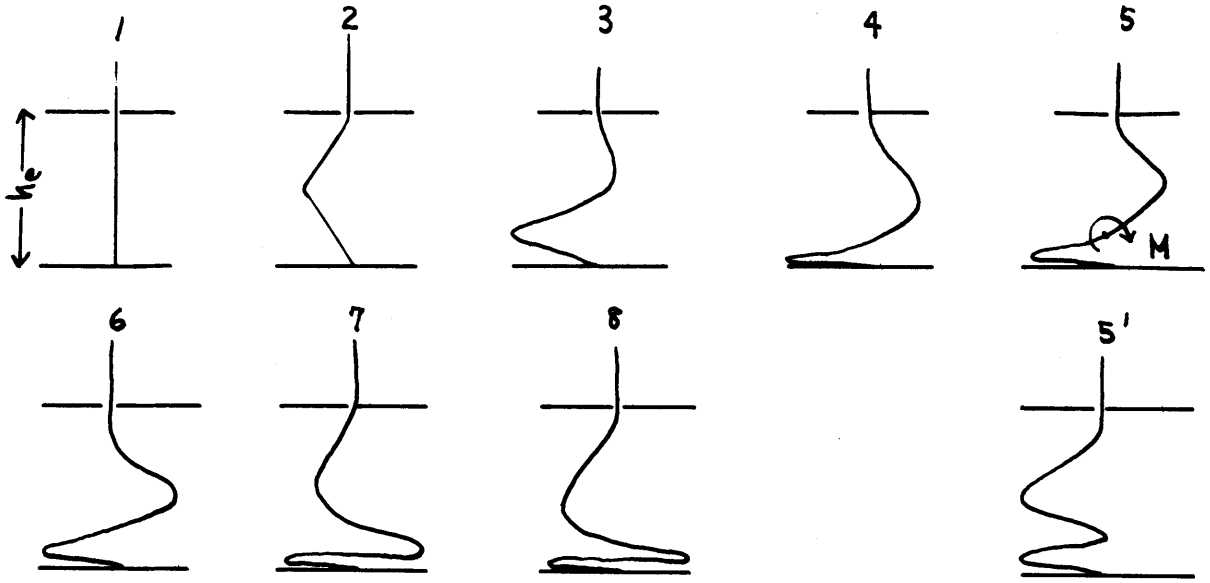

FIG. 37 Model of Buckling in Crimp Mechanism

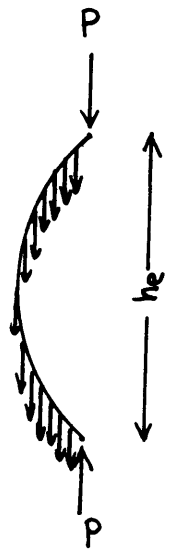

FIG. 38 Model of Buckling Being Affected by Inertia Force

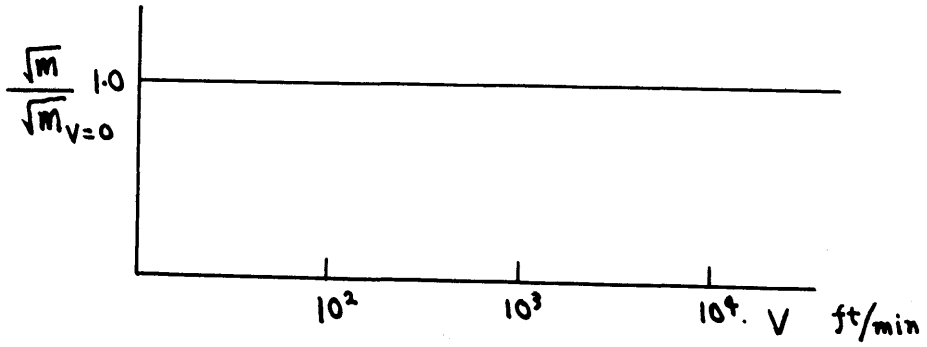

FIG. 39 EFFECT OF VELOCITY

$$\left.\begin{aligned} EIy'' &= -M \\ M &= P_s y - M_b \\ \frac{dM}{ds} &= P_s \frac{dy}{ds} + \int_0^s f_e \, ds \cdot \frac{dy}{ds} \end{aligned}\right\} \quad (3)$$

Taking y'' as $\frac{d\theta}{ds}$, and $\frac{dy}{ds} = \sin\theta$,

(4)

togetherwith the boundary conditions

$$\frac{d\theta}{ds} = 0 \quad \text{and} \quad \theta = \alpha \qquad (5)$$

This should be solved numerically. When P_s is the only acting force, the case is solved in Timoshenko's book.[16)]

3-1-2. Formation of Foundation

Recalling FIG.26 and 27, FIG.30 to FIG.35, the formation of the foundation, which is the essential determining stage of the crimp length l_c, can be devided into the two regions, the first is the very tip of the foundation where the primary fluctuation takes place, the second the delta region of the foundation where the secondary fluctuation initiates.

3-1-2-1. Very Tip of Foundation

In this small region, the crimped yarn constituting the planes parallel to the roll axis, is piling up as shown in FIG,27. Since every triangle is so close each other and the gap between the two rolls is so small, these planes act like rigid planes to the vertical pressure P_s, interacting each other through their frictional forces between the boundaries. This is very similar to the fluid motion between the plates

under the constant pressure. Since the diameter of the yarn is so small, the analogy between the velocity in the fluid and the displacement of the plane layer system seems to be reasonable as shown in FIG.42. In the laminar flow of Poiseulle flow[17],

$$V_x = -\frac{1}{2\eta}\frac{dP}{dx}(y_o^2 - y^2)$$

$$V_{x_{max}} = V_x(y=0) = -\frac{1}{2\eta}\frac{dP}{dx}y_o^2 \qquad (6)$$

where η is viscosity of the fluid.

From the equation (6)

$$h_e = l_c \propto \left(\text{const} - \frac{y_o^2}{"\mu"} \cdot P_s\right) \qquad (7)$$

$$= f("\mu", P_s, \text{geometry})$$

where "μ" is the effective shear force(lb/in), which could possibly be changed by the wedge action from the periphery of the roll. Since the buckling mechanism necessitates some definite space, we get from FIG.42

$$\left.\begin{aligned} &R_1(1-\cos\theta_1) = R_2(1-\cos\theta_2) \\ \text{and}\quad &\frac{P_s}{P_N} = \sin\theta \quad , \quad "\mu" \propto P_N \end{aligned}\right\} \qquad (8)$$

Therefore

$$h_e = l_c \propto (\text{const.}_1 - \text{const.}\sin\theta) \qquad (9).$$

The behavior of the primary fluctuation itself is considerably dependent on velocity V and possibly on μ and geometry. As

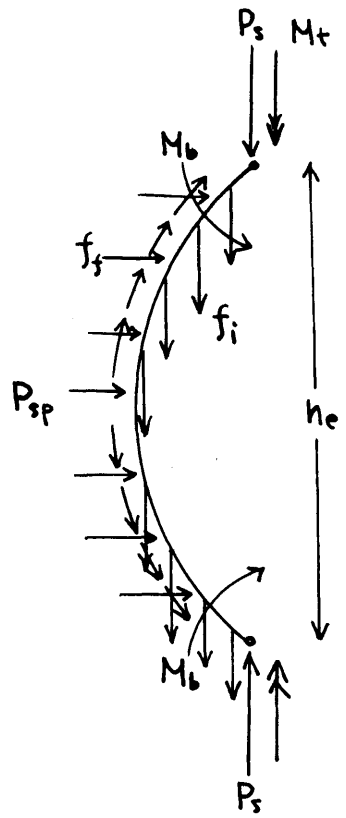

FIG.40 Buckling Model in General

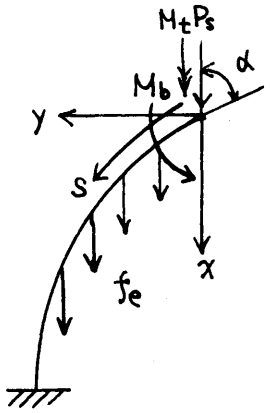

FIG.41 Simplified Model

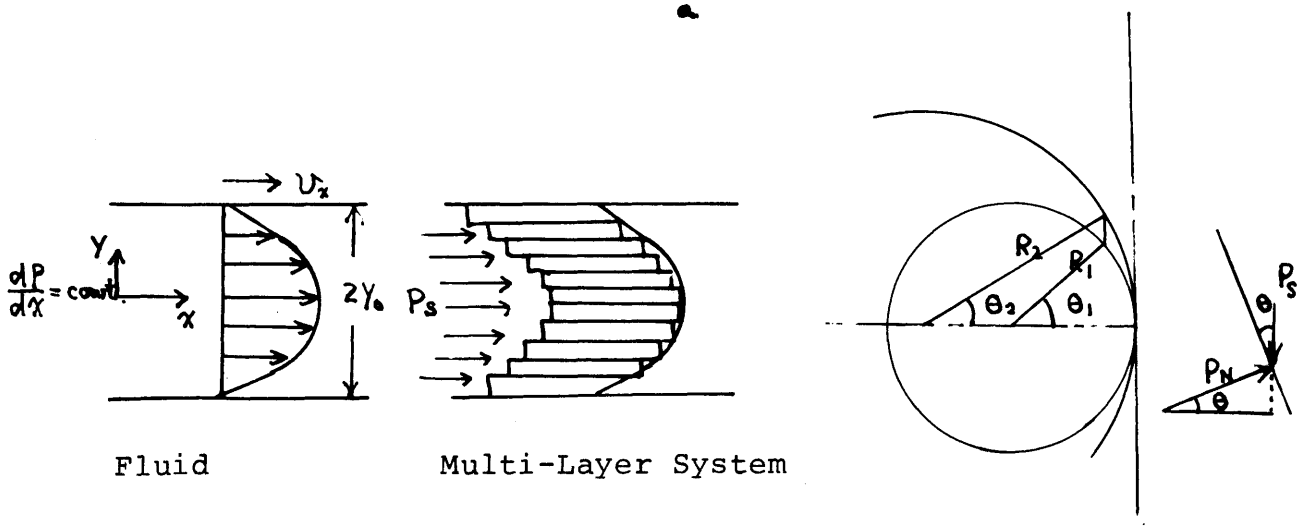

Fluid Multi-Layer System

FIG.42 Model for Analysing Tip Deformation

velocity increases the fluctuation becomes rather irregular and the fact could be compared with the fact that when the water jet impinges the plane, the increasing velocity makes the shape of the radial out-flow from the center turbulent and irregular. This irregularity is the essential defect of this mechanism and is so complicated that the only thing we can is to assume some distribution function for this effect.

3-1-2-2. Delta Region of Foundation

The behavior of the fiber assembly of this region can possibly influence the variation of the crimp length l_c. The various affecting factors are discussed in order.

3-1-2-2-1. Effect of Yarn Velocity V:

The velocity of the in-coming yarn V affects the geometry of the foundation in the following two respects; 1) inertia force, 2) frictional force between the planary layers which consist of the crimped yarns.

1) In-coming yarns impinge on the tip of the foundation while the yarns themselves twist and buckle successively, therefore this inertia force tends to deform the shape of the tip of the foundation. This effect may be represented by

$$l_c \propto F_i(V) = \alpha \rho V^2 \qquad (10)$$

2) A schematic model for the tip formation of the foundation is shown in FIG.43. Each layer, which consists of the crimped yarn, slips each other under the influence of the frictional

force due to the stuffing box pressure P_s. This relative slipping motion can be modeled as shown in the lower figure of FIG.43. Consequently the lowest layer has a kind of tension similar to the surface tension in the fluid. This tension T_e should balance the frictional force along the surface of the roll in a quasi-stable condition. This mechanism can lead to the following model, i.e., the problem of a suspension taut string under the uniform load P_s per unit length in FIG.44.

The well-known governing equation is

$$\frac{d^2y}{dx^2} = -\frac{P_s}{T_e} \tag{11}$$

togetherwith $y=0$ at $x=0$

$y=0$ at $x=l$

At the mid-point $x=l/2$,

$$y_{max} = \frac{P_s l^2}{4T_e} \tag{12}$$

Reconsidering the relative slipping motion, this is essentially equivalent to that in the drafting process. Since a great deal of attentions were paid to the drafting mechanism in the textile industry and many investigations wre accumulated, it seems to be natural to use some of those results. Typical results with respect to the friction-velocity relationships are [18]

$$F = (a_1 + a_2 V + a_3 V^2) \tag{13}$$

$V < 90$ ft/min

$$F = b - c\exp(-V) \doteqdot (b_1 + b_2 V - b_3 V^2) \tag{14}$$

$V < 60$ ft/min

Equation (14) shows that the frictional force varies at lower velocity but gradually approaches to the constant asymptotic value. Since the crimp length l_c is proportional to the geometrical length l_g, from the equation (12)

$$h_e = l_c \propto l_g - y_{max} = l_g - P_s l^2 / 4T_e \qquad (15)$$

In the quasi-equilibrium condition, T_e is comparable with the friction force in the drafting F, therefore

$$l_c \propto l_g - \frac{P_s l^2}{4(b_1 + b_2 V - b_3 V^2)} = F_f(V) \qquad (16)$$

Combining equation (16) with (10), a reasonable relationship between the crimp length l_c and the yarn velocity V is

$$l_c \propto c_1 + c_2 V - c_3 V^2 \qquad (17)$$

where c_1, c_2, and c_3 are all constants and positive numbers.

3-1-2-2-2. Effect of Geometry W,R, and Friction Coefficient μ:

A schematic view of the device under consideration is shown in FIG.45. In considering the force balance, the force contribution of the tip of the foundation can be neglected because of its tiny area. Furthermore the analysis is taken in the two dimensions, in other words, the side wall effect and inhomogeneity in the vicinity of the side wall are neglected. Taking some void region in one side into account, the equation of force balance is,

$$P_s W = \int_{\theta_1}^{\theta_2} (RF\cos\theta + RP_r \sin\theta)\, d\theta + \int_{\theta_1}^{\eta\theta_2} (RF\cos\theta + RP_r \sin\theta)\, d\theta$$

$$= P_r R \left\{ \int_{\theta_1}^{\theta_2} (\mu\cos\theta + \sin\theta)\, d\theta + \int_{\theta_1}^{\eta\theta_2} (\mu\cos\theta + \sin\theta)\, d\theta \right\} \quad (18)$$

where $\eta = \frac{\theta_3}{\theta_1}$ $\qquad 0 \leq \eta \leq 1$

Rearranging

$$\frac{P_s \cdot W}{2 P_n R\sqrt{1+\mu^2}} = \left[\cos\frac{1-\eta}{2}\theta_2 \sin\left(\frac{1+\eta}{2}\theta_2 - \beta\right) - \sin(\theta_1 - \beta) \right] \quad (19)$$

where $\tan\beta = 1/\mu$

Therefore

$$l_g = R\sin\theta_1 = R\sin\left[\beta + \sin^{-1}\left\{ \cos\frac{1-\eta}{2}\theta_2 \sin\left(\frac{1+\eta}{2}\theta_2 - \beta\right) - \frac{P_s W}{2 P_n R\sqrt{1+\mu^2}} \right\} \right] \quad (20)$$

Finally using a geometry $W = 2R(1 - \cos\theta_2)$,

$$l_g = f(R, \mu, \eta, W)$$

$$= R\sin\left[\left[\beta + \sin^{-1}\left[\cos\frac{1-\eta}{2}\left\{\cos^{-1}\left(1 - \frac{W}{2R}\right)\right\} \sin\frac{1+\eta}{2}\left\{\cos^{-1}\left(1 - \frac{W}{2R}\right) - \beta\right\} - \frac{P_s W}{2 P_n R\sqrt{1+\mu^2}} \right] \right]\right] \quad (21)$$

This equation shows the general tendencies,

as W increases l_g decreases

as R increases l_g increases

and l_g are not simply related,

where P_s / P_r is assumed to be a constant in a way.

3-1-2-2-3. Effect of Bending Rigidity EI and Stuffing Box

Pressure P_s :

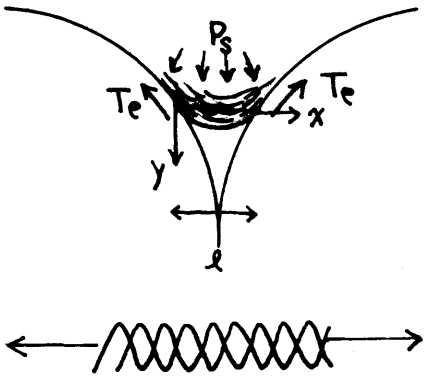

FIG.43 Schematic View of Tip in the Delta Region

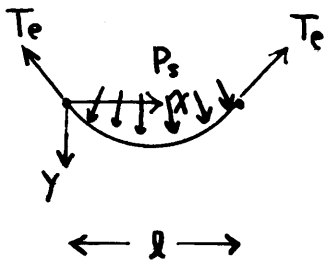

FIG.44 Simulated model of Tip

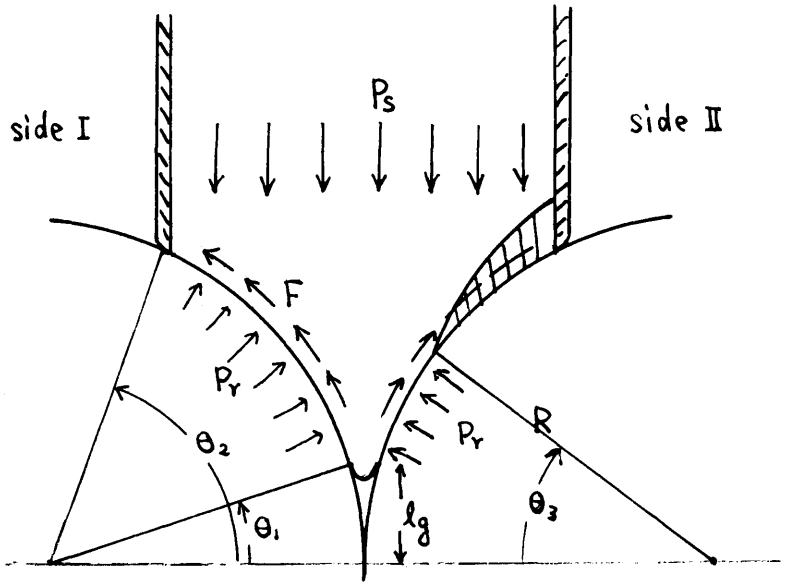

FIG.45 Analysis of Geometrical Effect

There seem to be two different approaches; the first introduces the idea of compressibility of the fiber assembly, the second is from the point of multi-layers system taking friction force into consideration. The actual mechanism is so complicated the combination of these two approaches may give a reasonable analysis.

1) Compressibility of Fiber Assembly:

The idea is as follows; if we could know the compressibility (equivalent to Bulk Modulus) 0f the foundation, the distance which the tip of the foundation will squeeze into the narrow region between the two rolls should be predictable. In other words, assuming the homogeneity of the fiber assembly and using the elastic relation between Bulk Modulus and elastic one dimensional strain, the distance of squeeze-in should be estimatable.

One of the earliest investigations in this area was undertaken by Van Wyk [19] in 1946 and several analyses were later initiated especially in Japan [20]. Although all the analyses sofar were based on a one- dimension model, a few of them seem to have good insight into the real situations caused by the complexity of the fiber assembly.

Looking at the situation where the fiber assembly is compressed by a load on the table one-dimensionally, the assumption is made that every fiber crosses the other fibers in the fiber assembly, forming a kind of net. The compression mecha-

nism is considered to be the case in which each element acts like a simple supported elastic beam with a concentrated load at the mid-point as shown in FIG.46. The distance between the cross points is considered as one unit, and defined as element length l_e. Therefore one half of the span length of a simply supported beam is equivalent to l_e. With help of Strength of Materials, the deflection δ at the mid-point due to load W_L is

$$\delta = l_e^3 \, W_L / 6EI \qquad (22)$$

If we consider this beam as one unit, the load W_L can be replaced by pressure P_s, the deflection by strain ϵ_L. Therefore a small increment of pressure dP_s and that of strain $d\epsilon$ are connected by

$$dP_s = \frac{6EI}{l_e^3} d\epsilon \qquad (23)$$

and this integration will lead to the equation of compression of the fiber assembly.

But the element length l_e will change in the process of the compression phenomenon. This can be reasoned as follows; at a state of no-load let the number of the elements in the fiber assembly N_o and at a certain stage N. Then the increment of the number dN as the height of the fiber assembly is reduced as much as dx under the one-dimensional load is approximated by

$$dN = -N \, U(x) \, dx \qquad (24)$$

In the present analysis U(x) is considered as a constant since we consider the one dimensional small change. And

$$(H_o - x)/ H_o = \varepsilon$$

where H_o is a initial height of the assembly, hence

$$-dx = H_o \, d\varepsilon \tag{25}$$

Substituting equation (25) into equation (24) and integrating with the initial condition $N = N_o$ at $\epsilon = 0$,

$$N = N_o e^{U H_o \varepsilon} \tag{26}$$

Furthermore, the inversely proportional relation is assumed,

$$\frac{1}{e} = \frac{C_1}{N_o} e^{-U H_o \varepsilon} \tag{27}$$

where C_1 is a constant.

Finally we get

$$dP_s = \frac{6 E I N_o^3}{C_1^3} e^{3 U H_o \varepsilon} \, d\varepsilon. \tag{28}$$

or

$$P_s = \frac{2 E I N_o^3}{U H_o C_1^3} \left(e^{3 U H_o \varepsilon} - 1 \right) \tag{29}$$

Now this equation is applied for our problem. Although in the actual case the boundary of the fiber assembly consists of the two circular arcs, this small region can be approximated as the one shown in the above figure of FIG.47. By the small increment of pressure dP_s, the assembly suffers a small strain $d\varepsilon$ according to the equation (28).

Since at the bottom the pressure is essentially zero, the middle portion of the assembly in the neighborhood of the bottom

has a tendency to reduce its strain energy, i.e., to bulge out from the original position. Hence the bulge-out distance is considered to be proportional to its strain ε.

That is

$$\frac{1}{3UH_0}\log\frac{UH_0C_1^3}{2N_0^3}\cdot\frac{P_s+1}{EI}=\varepsilon$$

Hence

$$l_c \propto l_g-\varepsilon = l_g+\frac{1}{3UH_0}\log EI\Big/\left[(P_s+1)\frac{UH_0C_1^3}{2N_0^3}\right]$$

$$= l_g + A\log\frac{EI}{B(P_s+1)} \qquad (30)$$

2) Multi-layer System Approach:

It was observed in the experiment that the building-up mechanism can be schematically shown as in FIG.48. Then the small region of the tip of the foundation could be approximated by a simply supported multi-layer beam with uniform load P_s in the two dimension as shown in the lower figure of FIG.48. This kind of analysis has led to the following general governing equation [21],

$$V = N"EI"\frac{dK}{dx}+\frac{h}{2}\sum_{i=1}^{N}(f_{i+1}+f_i) \qquad (31)$$

where

V ; over-all shearing force

N ; number of layers

"EI" ; equivalent bending rigidity

K ; curvature of the center line

y, x ; space coordinates

h ; height of a layer

f_i ; frictional force on the bottom of i-th layer

; coefficient of friction

P_{i+1} ; normal pressure on the top of i-th layer

For a good approximation in this bent shape, the normal pressure can be considered to vary linearly from P_s at the top layer to zero at the bottom layer [22] and so is the frictional force $f_i = \mu P_i$.

Equation (31) becomes

$$P_s x = N \text{"EI"} \frac{d^3y}{dx^3} + \frac{h}{2} \frac{\mu P_s}{N} \sum_{j=1}^{N} (2j-1)$$

$$= N \left[\text{"EI"} \frac{d^3y}{dx^3} + \frac{h}{2} \cdot \frac{\mu P_s}{N^2} \left\{ N(N+1)-1 \right\} \right] \quad (32)$$

$$\doteqdot N \left[\text{"EI"} \frac{d^3y}{dx^3} + \frac{\mu h}{2} P_s \right] \quad \text{when } N \gg 1 \quad (33)$$

Solving this equation (33) togetherwith

$$y = 0 \qquad \text{at } x = 1/2$$

$$\frac{dy}{dx} = 0 \qquad \text{at } x = 0$$

$$\frac{d^2y}{dx^2} = 0 \qquad \text{at } x = 1/2$$

$$y = \frac{\mu P_s}{24 \text{"EI"} N} x^4 + \frac{\mu h P_s}{12 \text{"EI"}} x^3 + \frac{C_1}{2} x + C_3 \quad (34)$$

the defection of the mid-point (at x= 0) is

$$\delta = c_3 = \frac{\mu P_s}{\text{"EI"}} \left[\frac{l^4}{N} \cdot \frac{5}{384} - \frac{h l^3}{96} \right] \quad (35)$$

Hence,

$$l_c \propto l_g - \delta = l_g - A_1 \frac{\mu P_s}{\text{"EI"}} \quad (36)$$

Next the equivalent bending rigidity "EI" is analysed. The following assumptions are made; 1) the configuration of

the crimped yarn is zig-zag, that is, of repeating triangles, 2) the crimped yarns lie in a plane, 3) the weight of yarn is negligible. Referring to FIG.49 we consider one unit of the layer, a triangle ABC. At points A, C, moment M is applied as shown by doubled arrows. Seperating $\overline{AB}$ and taking components of M along the direction of $\overline{AB}$ and perpendicular to $\overline{AB}$, M_t is a twisting moment and M_b is a pure bending moment as in FIG.50.

Then the deflection at the point B by the bending moment M_b is

$$\delta_B = \frac{M_b l_c^2}{2EI} = \frac{M \sin\varphi \, l_c^2}{2EI} \tag{37}$$

the twist angle is

$$\theta_B = \frac{M_t l_c}{G I_p} = \frac{M \cos\varphi \, l_c}{G I_p} \tag{38}$$

Now considering the deflection at the point C relative to that at the point B, deflection due to θ_B is

$$\delta_c' = l_c \theta_B \sin 2\varphi = \frac{2M \sin\varphi \cos^2\varphi \, l_c^2}{G I_p} \tag{39}$$

By the bending moment M_b

$$\delta_c'' = \frac{M \sin\varphi \, l_c^2}{2EI} \tag{40}$$

Twist angle is

$$\theta_c = \frac{M \cos\varphi . l_c}{G I_p} \tag{41}$$

Recalling that this value of twisting exists at the point A already by the preceding unit, the total deflection from A to

C is $$\delta = 2\left[\frac{M \sin\varphi \cdot l_c^2}{2EI} + \frac{2M\cos^2\varphi \cdot \sin\varphi \cdot l_c^2}{G I_p}\right] \quad (42)$$

The equivalent bending rigidity "EI" is thus defined,

$$\frac{M(2l_c \sin\varphi)^2}{2"EI"} = 2Ml_c^2\left[\frac{\sin\varphi}{2EI} + \frac{2\cos^2\varphi \cdot \sin\varphi}{G I_p}\right]$$

therefore

$$"EI" = \frac{\sin\varphi}{\frac{1}{2EI} + \frac{2\cos^2\varphi}{G I_p}} \quad (43)$$

where G is a shear modulus normally with $G = K_3 E$, and I_p is moment of inertia and in case of a circular cross section $I_p = 2I$. Hence,

$$"EI" = EI\left[\frac{\sin\varphi}{\frac{1}{2} + \frac{\cos^2\varphi}{K_3}}\right] \quad (44)$$

Two approaches have been worked out so far and they have given the similar functions, i.e., $l_c = F("EI"/P_s)$ or $F(P_s/"EI")$. Generally speaking, the first approach, that from the viewpoint of compressibility of the fiber assembly, provides a measure for the bulge-out of the tip of the foundation and the second one, by simulating the actual system into the multilayer system, gives not only a measure for the bulge-out but also an approximate shape of the tip of the foundation. Furthermore using the following Taylor series

$$\log x = \frac{x-1}{x} + \frac{1}{2}\left(\frac{x-1}{x}\right)^2 + \frac{1}{3}\left(\frac{x-1}{x}\right)^3 + \ldots\ldots \quad (45)$$

$(x > 1/2)$

it will be found that the both equations (30) and (36) provide a same tendency for the dependence of the crimp length l_c on the pressure P_s and the bending rigidity "EI" in terms of $P_s/"EI"$.

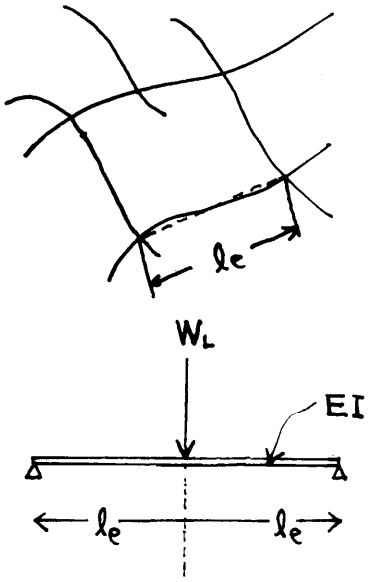

FIG.46 Elemental Unit in Fiber Assembly

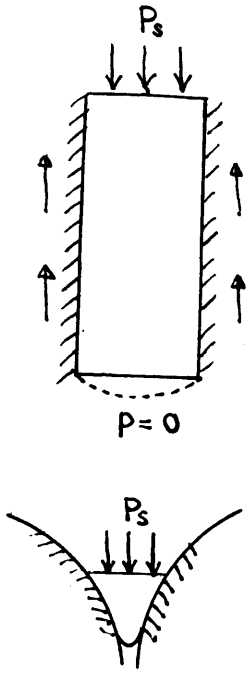

FIG.47 Bulge-out of Tip

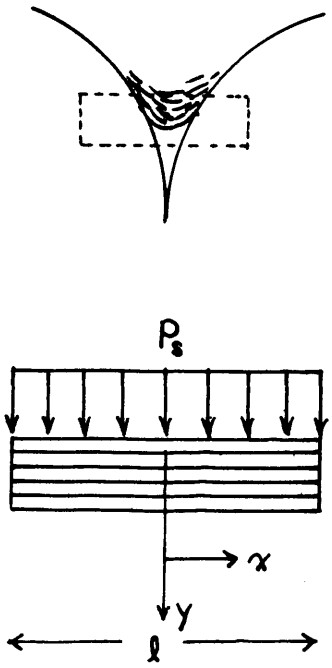

FIG.48 Modeled Multi-Layer Beam

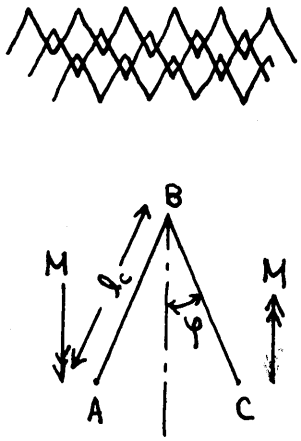

FIG.49 Bending Rigidity of Crimped Yarn Layer

3-1-2-2-4. Effect of Number of Filaments N:

Since the distance between the neighboring yarns are larger than the crimp length in case of monofilaments, the number of filaments contributes to smoothing out the irregularity of the primary fluctuation and this contribution is not too great. In the case of multi-filament yarns the filaments are very close each other, therefore this effective bending rigidity will be changed. Following the multi-layer system theory the actual bending rigidity is somewhere between $N(EI)_e$ and $N^2(EI)_e$, the former of which is the bending rigidity of a complete freedom motionconsideration and the latter is that of a no-freedom motion theory. Furthermore it is reasonable to assume that as P_s increases the effective bending rigidity of the multi-filaments comes closer to that of the no-freedom motion theory and this is indicated by the experimental result. Hence

$$"EI" = \alpha(P_s)(EI)_e \tag{46}$$

where $N < \alpha(P_s) < N^2$.

3-1-2-2-5. Effect of Nipping Pressure P_n :

Judging from the measurement of the flattening of the cross section, there is no considerable difference in the degree of the flattening, but it was observed that the total length of the flattened section per unit length is generally increased as P_n is increased. In the case of multifilament,

since there was no flattening effect this nipping pressure P_n does not contribute to the crimp lenght l_c as long as p_n is above the limit value which guarantees the positive feeding of the yarn.

3-1-2-2-6. Temperature Effect Temp :

As far as the crimp length is concerned, the temperature can affect Young Modulus E only and this E does influence the crimp length l_c through the characteristics of the fiber assembly (foundation). Therefore once Temp-E relation is given and the average temperature of the foundation is assumed, the previous analysis can give the answer.

3-2 Dimensional analysis

The previous qualitative analysis has led to the equations which give the relationships among the factors affecting the crimp length l_c. They are:

$$l_c \propto (\text{const}_1 - \text{const.}\sin\theta) \tag{9}$$

$$l_c \propto C_1 + C_2 V - C_3 V^2 \tag{17}$$

$$l_c \propto R \sin\left[\left[\beta + \sin^{-1}\left[\cos\frac{1-\mu}{2}\left\{\cos^{-1}\left(1-\frac{W}{2R}\right)\right\}\sin\left\{\frac{1+\mu}{2}x\right.\right.\right.\right.$$
$$\left.\left.\left.\left.\cos^{-1}\left(1-\frac{W}{2R}\right)-\beta\right\}-\frac{P_s W}{2P_r R\sqrt{1+\mu^2}}\right]\right]\right] \tag{21}$$

$$l_c \propto K_o + A \log\frac{EI}{B(P_s+1)} \tag{30}$$

or

$$l_c \propto K_1 - A_1\frac{\mu P_s}{"EI"} \tag{36}$$

In order to get the approximate and compact relationship in the non-dimensional form, the following procedures were carried out.

From the equation (9) using equation (8),

$$1 = f_c(R/R_1) \tag{47}$$

The equation (17) was actually derivated by the friction-velocity relation consideration, so that

$$1 = f_c(V \cdot d\mu/dV) \tag{48}$$

or more appropriately for the realistic purpose,

$$1 = f_c\left\{C_3 + C_1(V/V_o) - C_2(V/V_o)^2\right\} \tag{49}$$

To simplify the equation (21), we assume $\eta = 1$ and $\beta = \tan^{-1}\frac{1}{\mu}$ is constant then

$$1 = f_c(W/R) \tag{50}$$

The equations (30) and (36) togetherwith the elastic buckling theory, the following non-dimensional quantity is considered.

$$\frac{l_c^2 P_s d^2}{"EI"} \tag{51}$$

where d is a diameter of the fiber concerned.

Therefore the final form is

$$\frac{l_c^2 P_s d^2}{"EI"} = f_1(R/R)\, f_2(V d /dV)\, f_4(W/R) \tag{52}$$

Taking the probability function $P(R,EI,N,T,\mu)$, which relates the primary function, into consideration and combining f_1 and f_4,

$$\frac{l_c^2 P_s^2 d}{"EI"} = A_3 (W/R)^m (V\cdot d\mu/dV)^n P(R,EI,N,T,\mu) \quad (53)$$

or

$$\frac{l_c^2 P_s^2 d}{"EI"} = A_4 (W/R)^m \left\{ C_1 + C_2 (V/V_0) - C_3 (V/V_0)^2 \right\} x$$
$$P(R,EI,N,T,\mu) \quad (54)$$

where V_0 represents the standard velocity and T does the thickness of the roll.

If the density ρ is constant, in other words, as long as we are concerned with the same material, d and I are related with the yarn denier D as follows,

$$\begin{matrix} d^2 \propto D^2 \\ I \propto D^2 \end{matrix} \quad (55)$$

Therefore,

$$\frac{l_c^2 P_s}{E D} = A^* (W/R)^m \left\{ C_1 + C_2 (V/V_0) - C_3 (V/V_0)^2 \right\} x$$
$$P(R,EI,N,T,\mu) \quad (56)$$

Referring to FIG.51 and 52,

$$\frac{l_c^2 P_s}{D} = 1.85\times10^{-11} (W/R)^{-1.75} \left\{ 0.18+0.78(V/V_0) - 0.063x (V/V_0)^2 \right\} P(R,EI,N,T,\mu) \quad (57)$$

where the numerical quantities are taken as

$$E = 1.0 \times 10^{5} \ Kg/mm^{2}$$

$$\rho = 1.14 \ g/cm^{3}$$

CHAPTER 4 Conclusion

The complete analysis of the whole mechanism of the stuffing box crimper is so complicated, because there are a three dimensional buckling mechanism, a frictional behavior of the material with respect to crimp configuration and velocity, the characteristics of the fiber assembly which is also complicated, and visco-elastic properties of the material togetherwith the crystallization behavior under the stress and temperature effects. Nevertheless, by step-by-step careful observations and simulating experiment, the basic mechanism for the determination of the characteristic length of the crimped yarn l_c was made clear. The determining mechanism of the crimp angle θ_c was briefly discussed and left to the future research.

Simplifying and modeling the actual mechanism, the theoretical analysis has led to a good agreement with the experimental results and is finally put into the non-dimensional form. And as far as the experiments carried out are concerned the non-dimensional form is given quatitatively.

Summarising the obtained results;

1) The crimp mechanism is a successive rapid buckling in the small crucial region, an immediate neighborhood of the nipping point of the feed rolls.

2) The geometry of the crucial region is a determining factor of the crimp length l_c.

3) The relationships in the non-dimensional form are,

$$\frac{l_c^2 P_s d^2}{"EI"} = f_1(R/R)\, f_2(V\cdot d\mu/dV)\, f_4(W/R)\, P(R,EI,N,T,\mu)$$

or

$$\frac{l_c^2 P_s}{E D} = A^*(W/R)^m \left\{ C_1 + C_2 (V/V_0) - C_3 (V/V_0)^2 \right\} P(R,EI,N,T,\mu)$$

CHAPTER 5 Suggestions for Future Work

In this thesis the basic crimp mechanism for the stuffing box crimper was made clear. Nevertheless, due to the complexity of the crimping mechanism and its involvement with numerous sub-mechnisms the following investigatins are suggested to develop a more complete understanding of the whole crimping process.

1) Crimp Rigidity; this is naturally related to the crimp angle θ_c and should be studied from the stanpoint of viscoelastic behavior. For example, using a heavy denier monofilament the following investigation is suggested. First one unit of the crimp configuration is studied under the influences of temperature, time, crystallization, and relaxation behavior

as indicated schematically in the below figure.

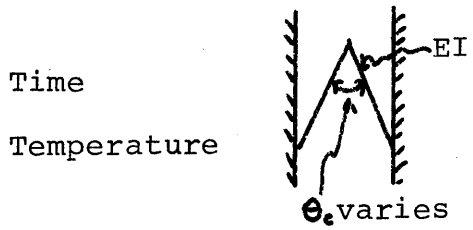

Independently pressure P_s - crimp angle θ_c in the fiber assembly should be studied statistically.

2) Probability function P; more detailed observation through the high speed movie camera is recommended to establish the statistical behavior of the piling up of the tip of the foundation.

3) Buckling of the multi-layer system; to extend these studies to the case of staple fibers, this investigation sould be carried out.

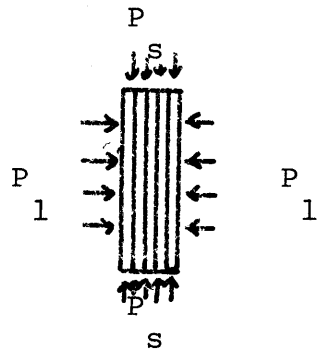

4) Frictional Behavior; under the several level of the lateral pressure, a study should be made of the μ vs V relation with respect to crimp configuration, denier and material.

This is closely related with the drafting mechanism except that

there is no positive lateral pressure.

BIBLIOGRAPHY

1 M.Horio&Kondo, "CRIMPING OF WOOL FIBER", Tex. R. J. June 1953, pp373

M.Horio&Kondo, "THEORY & MORPHOLOGY OF CRIMPED RAYON STAPLE" ibid. 1953, pp137

2 U.S.P. 332,514, U.S.P. 332,515

U.S.P. 1,353, 337

3 U.S.P. 568,052

4 U.S.P. 2,409,066

5 U.S.P. 2,514,557, U.S.P. 2,575,833-839

6 " PATTERN & PROBLEMS OF TECHNICAL INNOVATION IN AMERICAN INDUSTRY", Report to National Science Foundation, PB181573, 1963,' pp43

7 U.S.P. 2,734,228, U.S.P. 2,854,728, etc.

8 W.Morawek, "NEUERSTER STAND DER TEXTURIERTECHNOLOGIE", Textil Praxis, Vol.20, 1965, pp793

Textil Praxis, International, No.4 1965, pp181

9 Kimura, J of Textile Machinery Society, Japan, Vol.17 1964, pp330

10 U.S.P. 2,439,814, U.S.P. 2,439,815

11 U.S.P. 2,931,091, U.S.P. 2,988,420

12 Brand & S.Backer, "MECHANICAL PRINCIPLE OF NATURAL CRIMP OF FIBER", Tex. R. J. 1962, pp39

13 K.Kawasaki, J of Tex.Mach. Soc. Japan, Vol.16 1963, pp37

14 K.Sasaki & Y.Ishikawa, ibid, Vol.14, 1961,pp61

15 N.W.Mckillop, Canadian Textile Journal, April, 1965, pp61

16 Timoshenko, " THEORY OF ELASTIC STABILITY", 1961ed., pp76, pp107

17 W.Rohsenow, H.Choi, "HEAT, MASS, AND MOMENTUM TRANSFER", 1963ed., pp34

18 H.G.Howell, et al, " FRICTION IN TEXTILE", i959ed.

19 C.M.van Wyk, J. T. I. Vol.37, 1946, T285

20 Wakayama, Hattori, J of Tex. Mach. Soc., Japan, 1958, pp167

21 Peter Popper, Ph D Thesis at M.I.T. June, 1966

22 N.Kouguchi, Unpublished Term Paper, January, 1966

APPENDIX 1

Captions of Tables and Figures, and Their Location

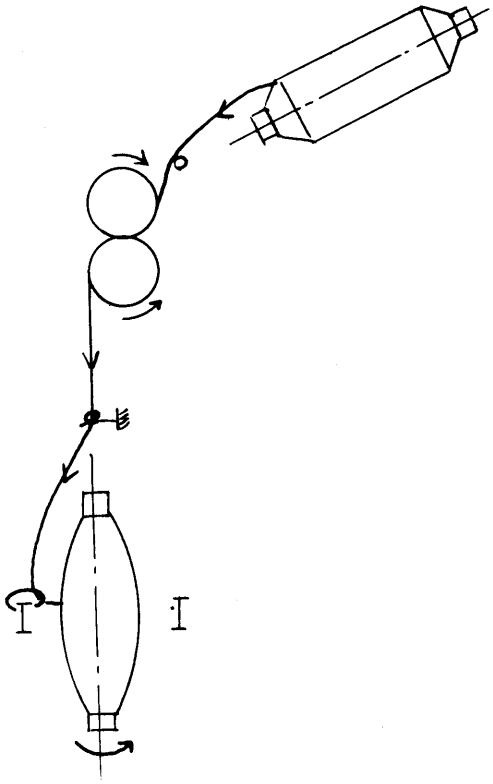

FIG.1 CONVENTIONAL METHOD

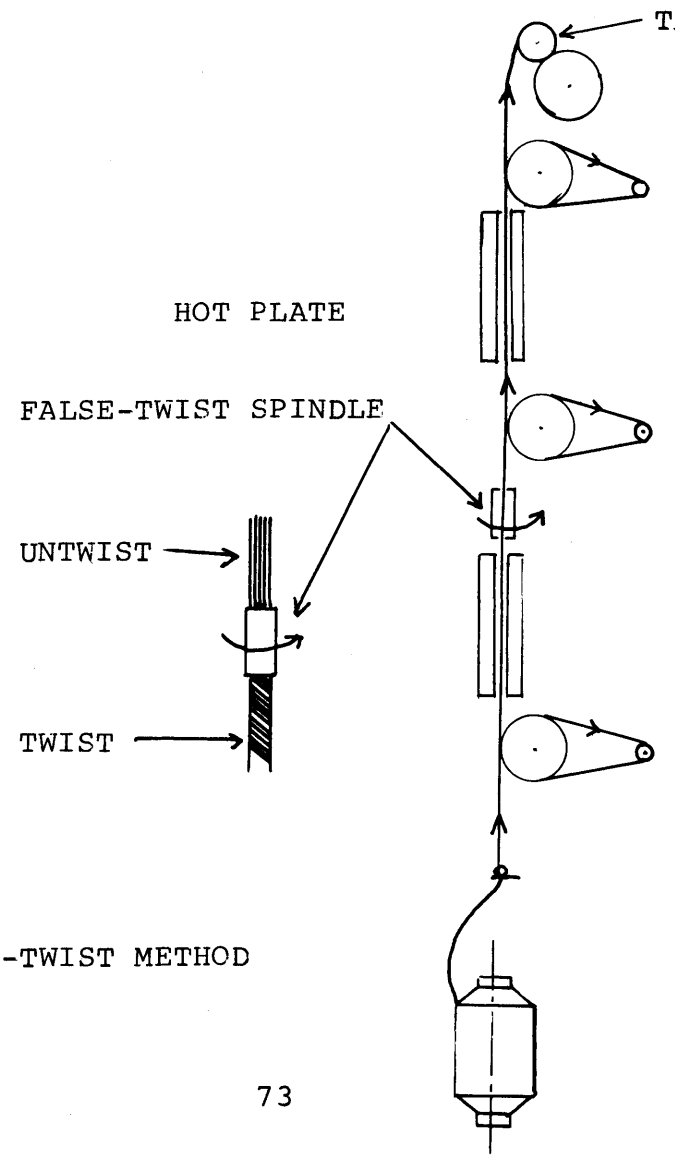

FIG.2 FALSE-TWIST METHOD

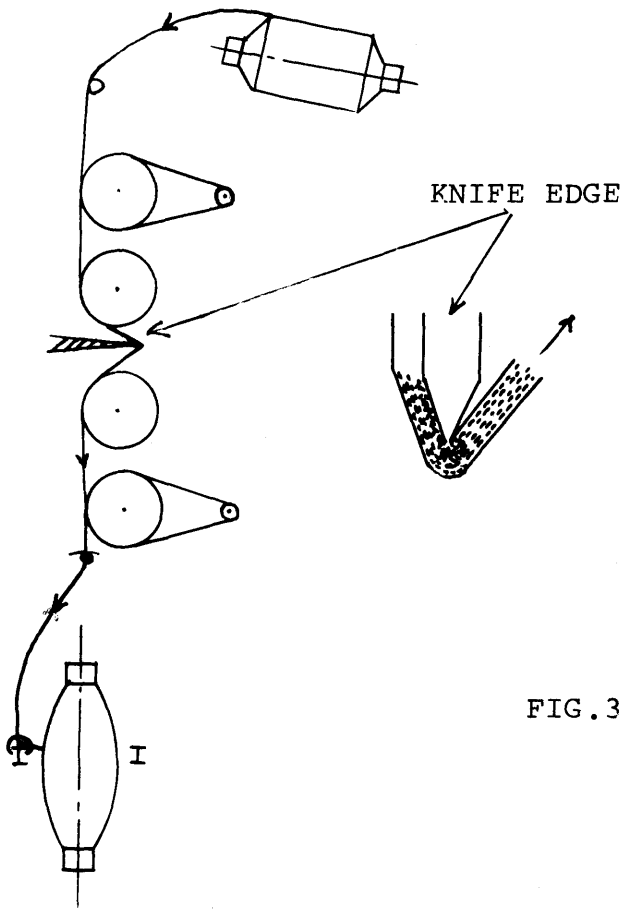

FIG.3 EDGE CRIMPING METHOD

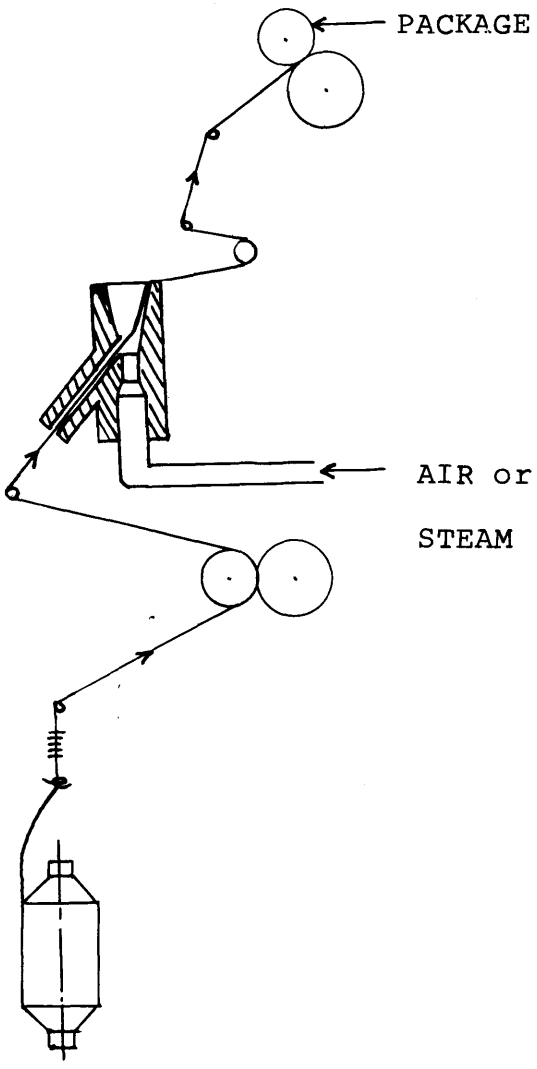

FIG. 4 AIR-JET or
STEAM-JET METHOD

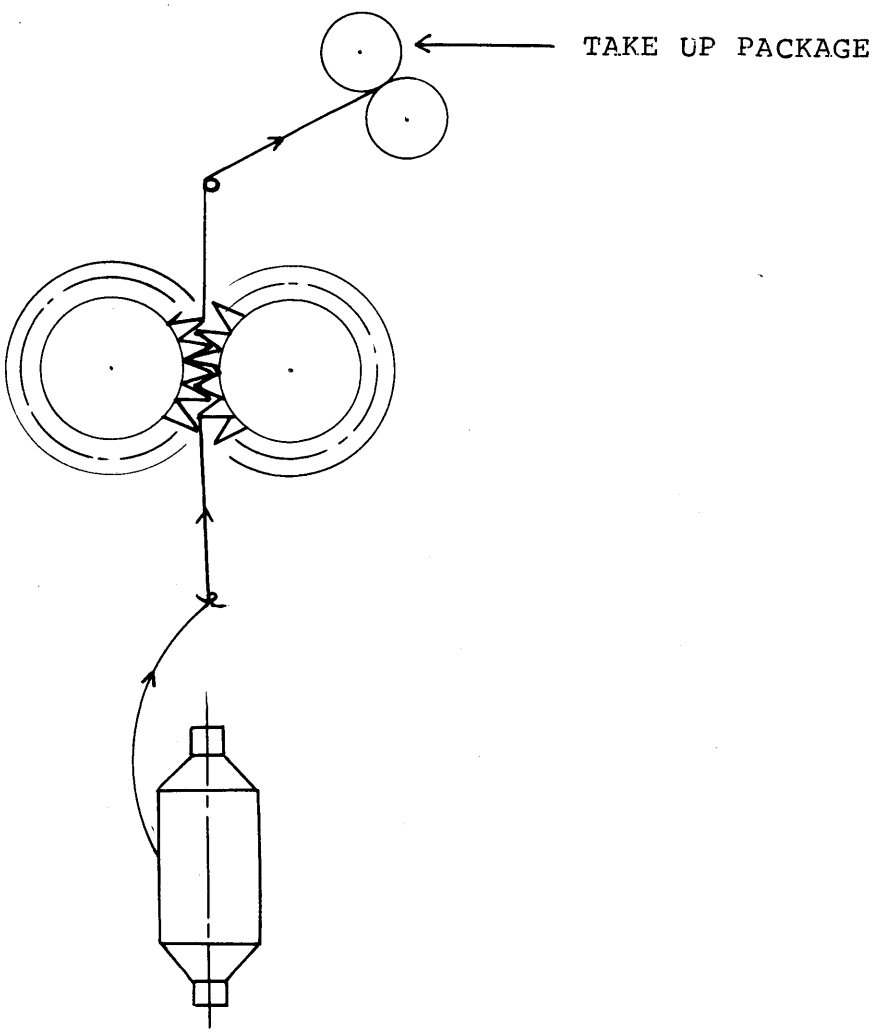

FIG. 5 GEAR CRIMPING METHOD

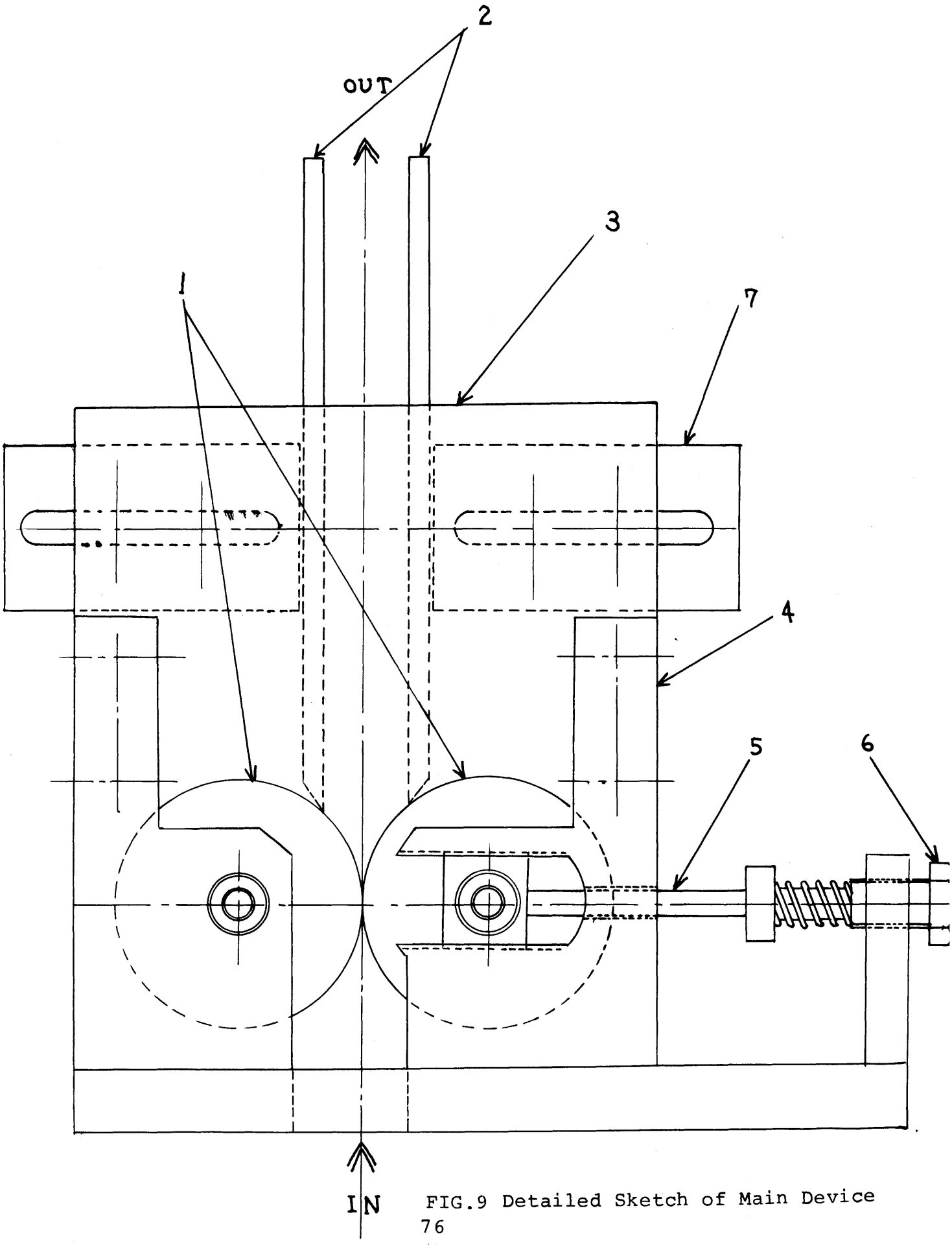

FIG.9 Detailed Sketch of Main Device

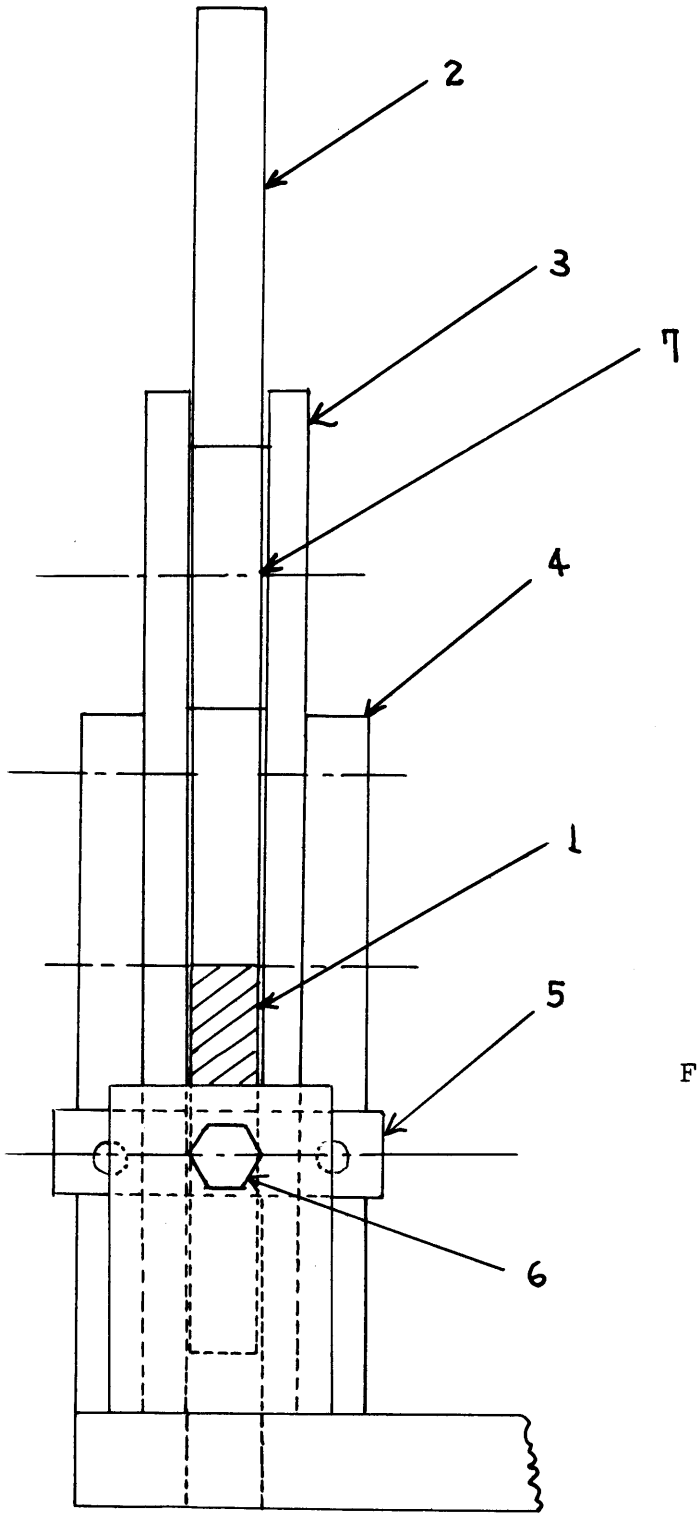

FIG. 10 SIDE VIEW OF FIG. 9

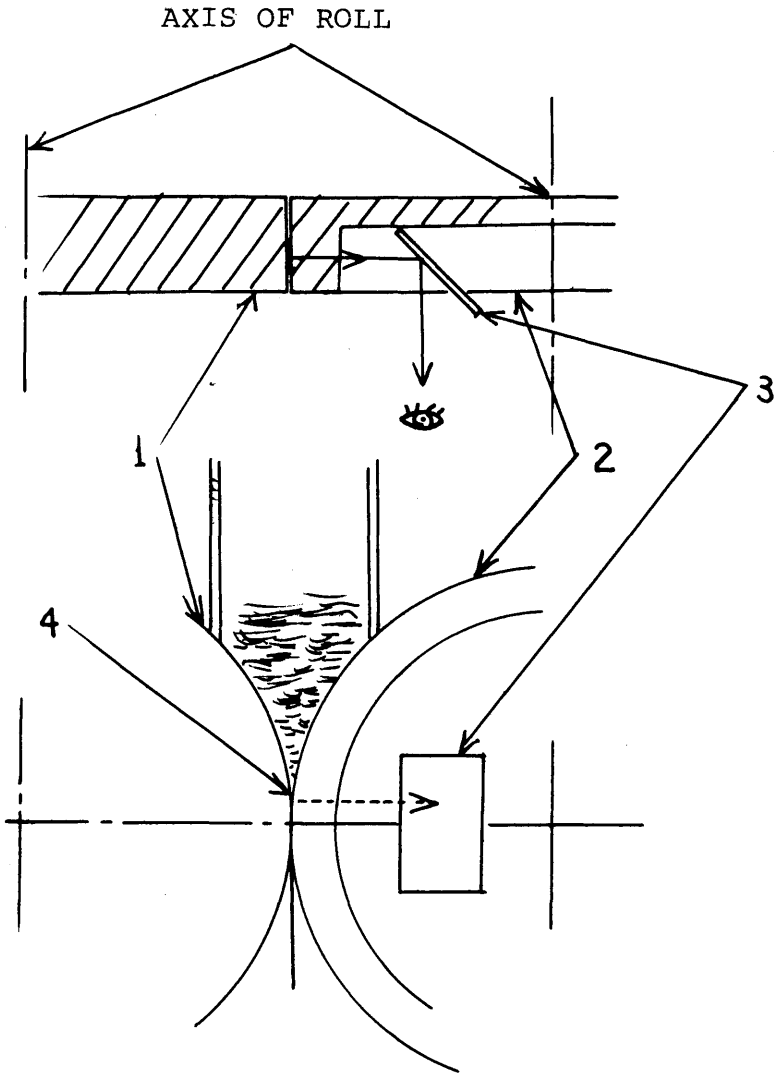

FIG. 11 Special Device for Observation of Crucial Region

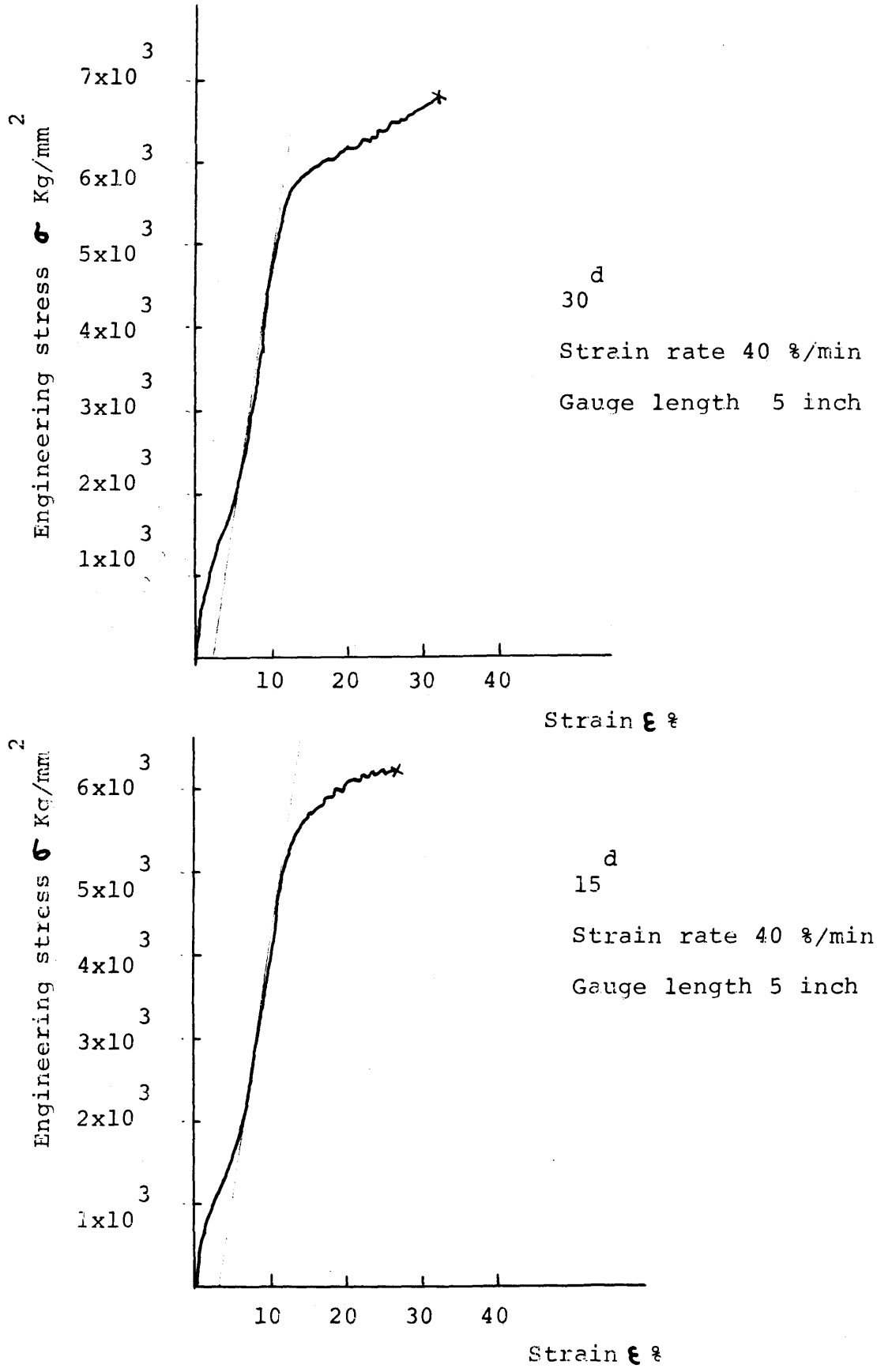

FIG. 17 STRAIN-STRESS CURVE

Table 3 Design of Experiment

Group 1 D W N R t P (fixed)
2 1 1 1 1 n2

P V	P V	P V
s11 l1	s11 l2	s11 l3
P V	P V	P V
s12 l1	s12 l2	s12 l3
P V	P V	P V
s13 l1	s13 l2	s13 l3

Group 2 D N R V t P (fixed)
2 1 1 l2 1 n2

P W	P W	P W
s11 1	s12 1	s13 1
P W	P W	P W
s21 2	s22 2	s23 2

Group 3 D R V W t P
2 1 l2 1 1 n2

P N	P N	P N
s11 1	s12 1	s13 1
P N	P N	P N
s11 2	s12 2	s13 2
P N	P N	P N
s11 3	s12 3	s13 3

Group 4 N W R V t P (fixed)
2 1 1 l2 1 n2

P D	P D	P D
s11 1	s12 1	s13 1
P D	P D	P D
s11 2	s12 2	s13 2
P D	P D	P D
s11 3	s12 3	s13 3

Group 5 D V N W t P (fixed)
2 12 2 1 1 n2

P R P R P R
s11 1 s12 1 s13 1

P R P R P R
s11 2 s12 2 s13 2

D V N W t P (fixed)
2 12 2 2 1 n2

P R P R P R
s21 1 s22 1 s23 1

P R P R P R
s21 2 s22 2 s23 2

Group 6 V D P W R t (fixed)
12 3 s12 1 1 1

P P P
n1 n2 n3

Group 7 D P W R N t P (fixed)
m s12 1 1 m 1 n2

V V V V
11 12 13 14

Group 8 V D W R N t P (fixed)
12 m 1 1 m 1 n2

P P P
s11 s12 v s13

Table 3

GRUOP]

V	D	P_s	W	R	N	t	P_n
	2		]	]	]	]	2

	$P_{s]]}V_{]]}$	$P_{S]]}V_{]2}$	$P_{s]]}V_{]3}$	$P_{s]2}V_{]]}$	$P_{s]2}V_{]2}$	$P_{s]2}V_{]3}$
]	6.50	]0.]]*	8.65	5.00	6.54	5.60 *
2	6.58 *	9.49 *	8.00 *	4.36	7.35 *	3.40
3	8.00	8.00	8.50 *	5.44 *	6.]8	4.]9
4	8.08	]0.00*	8.50 *	5.2] *	7.3] *	3.85
5	7.90 *	8.34	6.50	4.78	7.55 *	6.66
6	7.35 *	8.78	8.50 *	5.69 *	7.65 *	5.2] *
7	7.00 *	9.00 *	8.50	7.62	7.45 *	6.45 *
8	6.]]	]].73	6.20	5.72 *	8.00	6.00 *
9	8.00	]0.00 *	8.00 *	6.]0 *	8.2]	5.85 *
]0	7.28 *	]0.80	8.50	6.70	8.25	7.35
$X_{]0}$	7.28	9.63	7.99	5.66	7.50	5.46
Σ 5	36.]]	48.60	4].50	28.]6	37.3]	29.]]
X_5	7.22	9.72	8.30	5.63	7.46	5.82
	x 0.087					
l_c	.627	.846	.722	.490	.649	.506

Table 4

GROUP](continued)

	$P_{s]3}V_{]]}$	$P_{s]3}V_{]2}$	$P_{s]3}V_{]3}$
]	5.00	5.73 *	5.90 *
2	5.78 *	5.45	5.54
3	5.46 *	7.]4	7.8]
4	5.24 *	5.64 *	5.60 *
5	7.55	6.]6	5.4]
6	7.00	5.64 *	6.24 *
7	4.50	5.70 *	6.40 *
8	6.00 *	5.00	6.50
9	5.05	6.25 *	5.46
]0	5.47 *	7.4]	6.00 *
$X_{]0}$	5.7]	6.0]	6.08
Σ 5	27.95	28.96	30.]4
X_5	5.59	5.79	6.03
	xo.087		
l_c	.487	.503	.524

Table 4

GROUP 2

V	D	P_s	W	R	N	t	P_N
]2	2			]	]	]	2

	$P_{s]]}W_]$	$P_{s2]}W_2$	$P_{s]2}W_]$	$P_{s22}W_2$	$P_{s]3}W_]$	$P_{s23}W_2$
]		9.36		6.00 *		5.48
2		7.56 *		5.64		4.29
3		9.34		8.00		4.68 *
4		7.75 *		7.90		4.68 *
5		7.30		7.00 *		4.26
6		8.00 *		5.65		5.00 *
7		7.]8		7.23 *		4.99 *
8		8.87		6.70 *		5.90
9		8.30 *		5.60		4.]0
]0		8.25 *		7.00 *		5.]2 *
$X_{]0}$		8.]9		6.67		4.85
Σ 5		39.86		33.93		24.48
X_5		7.97		6.79		4.90
	x 0.087					
l_c	.846	.693	.649	.59]	.503	.426

Table 5

GROUP 3

V	D	P_S	W	R	N	t	P_n
]2	2		]	]		]	2

	$P_{s]]}N_{]}$	$P_{s]]}N_2$	$P_{s]]}N_3$	$P_{s]2}N_{]}$	$P_{s]2}N_2$	$P_{s]2}N_3$
]		6.34	8.00 *		5.68	6.65
2		6.66 *	8.]0 *		5.50	8.00 *
3		7.00 *	7.80		5.70	7.00 *
4		6.70 *	9.60		6.45 *	8.2]
5		8.3]	8.2] *		7.54	7.02 *
6		7.00 *	8.20 *		6.48 *	7.76 *
7		6.60 *	7 50		7.]5 *	6.70
8		6.40	6.80		7.69	8.50
9		6.52	8.50 *		7.]] *	9.40
]0		8.00	8.99		6.]2 *	7.20 *
$X_{]0}$		6.95	8.]7		6.54	7.64
Σ 5		33.96	4].0]		33.3]	36.98
X_5		6.79	8.20		6.66	7.39
	xo.087					
l_c	.846	.59]	.7]3	.649	.579	.643

Table 6

GROUP 3(continued)

	$P_{s]3}N_{]}$	$P_{s]3}N_{2}$	$P_{s]3}N_{3}$
]		7.00 *	8.40
2		6.84 *	8.20
3		6.53	7.66 *
4		7.57 *	7.55 *
5		8.64	7.20 *
6		8.35	7.00
7		7.56 *	6.80
8		6.64	6.70
9		6.00	8.0] *
]0		7.25 *	7.59 *
$X_{]0}$		7.24	7.5]
Σ 5		36.23	38.0]
X_{5}		7.24	7.60
	x0.087		
l_{c}	.503	.630	.662

Table 6

GROUP 4

V	D	P_s	W	R	N	t	P_n
]2			]	]	2	]	2

	$P_{s]]}D_]$	$P_{s]]}D_2$	$P_{s]]}D_3$	$P_{s]2}D_]$	$P_{s]2}D_2$	$P_{s]2}D_3$
]	6.00 *		9.00	6.08 *		9.3]
2	5.00		]2.00	5.43 *		]0.4]
3	6.25 *		]0.95*	5.95 *		7.72 *
4	6.00		]0.00*	7.]8		9.00
5	6.68 *		]].05	6.38		7.00 *
6	7.04 *		]0.]0*	6.50		6.68 *
7	7.85		7.73	4.50		6.98 *
8	5.84		]0.95*	5.00 *		7.58 *
9	6.57 *		]].34	4.08		6.75
]0	7.85		]0.74*	4.99 *		6.75
$X_{]0}$	6.5]		]0.39	5.6]		7.83
Σ 5	32.54		52.74	27.46		36.]0
X_5	6.5]		]0.55	5.49		7.22
	x0.087					
l_c	.567	.59].....	.9]8	.478	.579	.628

Table 7

GROUP 4 (continued)

	$P_{s]3}D_{]}$	$P_{s]3}D_{2}$	$P_{s]3}D_{3}$
]	4.95		7.00
2	4.99 *		6.30
3	5.00 *		7.83
4	5.0] *		7.00 *
5	5.70		7.00 *
6	5.96		8.00
7	5.00 *		7.25 *
8	5.80		7.04 *
9	5.00 *		7.99
]0	4.90		7.00 *
$X_{]0}$	5.23		7.24
Σ 5	25.00		35.29
X_{5}	5.00		7.06
	x0.087		
^{1}c	.435	.630	.6]4

Table 7

GROUP 5

V	D	P_S	W	R	N	t	P_n
2	2		]		2	]	2

	$P_{s]]}R_{]}$	$P_{s]]}R_2$	$P_{s]2}R_{]}$	$P_{s]2}R_2$	$P_{s]3}R_{]}$	$P_{s]3}R_2$
]		9.]0		9.30		9.00
2		]].]4*		]0.50		]0.0]*
3		]0.00*		]0.20*		8.60
4		9.99 *		]0.20*		]].00
5		9.40		9.26 *		]0.50*
6		]2.00		9.0]		8.50
7		]].20*		]0.06*		]0.00*
8		]].00*		]].00		9.00 *
9		]0.00		9.00		]0.00*
]0		]2.50		9.80 *		]].00
$X_{]0}$		]0.63		9.83		9.76
Σ 5		53.34		49.54		49.50
X_5		]0.67		9.9]		9.90
	xo.087					
l_c	.59]	.928	.579	.862	.630	.86]

Table 8

GROUP 5(continued)

V	D	P_s	W	R	N	t	P_n
2	2		2		2	]	2

	$P_{s2]}R_]$	$P_{s2]}R_2$	$P_{s22}R_]$	$P_{s22}R_2$	$P_{s23}R_]$	$P_{s23}R_2$
]	9.00	]0.70	8.00	8.50	5.25	9.50 *
2	9.00	]].00	9.20	8.00	6.70 *	9.00 *
3	7.38 *	9.50 *	6.00 *	8.50 *	5.37 *	]0.00
4	7.80 *	9.40 *	5.69	8.00	5.00	9.00 *
5	9.40	]0.00*	7.20 *	9.60 *	5.78 *	]0.50
6	7.93 *	]].04	6.59 *	]2.00	5.23	8.00
7	7.80 *	9.20	5.00	9.80 *	6.24 *	9.60 *
8	8.84	9.00	6.70 *	9.00 *	6.68 *	9.00 *
9	7.79 *	9.50 *	5.89	8.70 *	6.75	8.00
]0	6.98	]0.20*	6.00 *	]].00	6.80	8.30
$X_{]0}$	8.]9	9.95	6.63	9.30	5.98	9.09
Σ 5	38.70	48.60	32.49	45.50	30.77	46.0]
X_5	7.74	9.72	6.50	9.]0	6.]6	9.2]
	x0.087					
l_c	.673	.846	.566	.792	.536	.800

Table 8

GROUP 6

V	D	P_s	W	R	N	t	P_N
]2	3	]2	]	]	]	]	

	$P_{n]}$	P_{n2}	P_{n3}
]	7.00	7.34	6.40 *
2	9.62	8.00 *	7.00 *
3	8.85 *	8.67	7.34
4	9.]2	8.0] *	6.85 *
5	8.45 *	7.]5	7.]5 *
6	7.95 *	6.65	7.65
7	7.35	7.35 *	6.00
8	7.47	8.]0 *	7.00 *
9	8.54 *	7.60 *	7.45
]0	7.50 *	8.25	6.00
$X_{]0}$	8.]8	7.7]	6.93
Σ 5	4].29	39.05	35.34
X_5	8.]6	7.58	7.07
	x0.087		
l_c	.7]0	.660	.6]4

Table 9

GROUP 7

V	D	P_s	W	R	N	t	P_n
	m	]2	]	]	m	]	2

	$V_{]]}$	$V_{]2}$	$V_{]3}$	$V_{]4}$
]	2.]9 *	3.35	3.00	4.00
2	2.34 *	2.55	2.95	3.59 *
3	].90	3.3]	3.5] *	2.90
4	2.]3 *	2.9] *	3.3] *	4.65
5	2.03	2.98 *	3.24 *	3.70 *
6	2.28 *	3.00	3.24 *	3.74 *
7	2.46	2.86 *	3.49	3.35 *
8	2.52	2.34	3.35 *	2.75
9	2.60	2.83 *	2.96	3.56 *
]0	2.47 *	2.97 *	3.64	2.80
$X_{]0}$	2.29	2.9]	3.27	3.50
Σ 5	]].4]	]4.55	]6.65	]7.94
X_5	2.28	2.9]	3.33	3.59
	x0.32			
1_c	.730	.932	].07	].]5

Table]0

GROUP 8

V	D	P_s	W	R	N	t	P_n
]2	m		]	]	m	]	2

	$P_{s]]}$	$P_{s]2}$	$P_{s]3}$
]	3.3] *	2.28	2.83
2	2.98	3.00	2.47 *
3	3.2] *	2.87 *	2.29 *
4	2.85	2.68 *	2.4] *
5	3.26 *	2.]5	].95
6	2.86	3.]5	2.]6 *
7	3.09 *	2.75 *	2.]]
8	3.55	2.97 *	2.70
9	3.]5 *	2.85 *	2.58 *
]0	3.5]	2.47	2.]9 *
$X_{]0}$	3.]8	2.72	2.37
Σ 5	]6.02	]4.]2	]].94
X_5	3.20	2.82	2.39
	x.32		
l_c	].024	.903	.765

Table]]

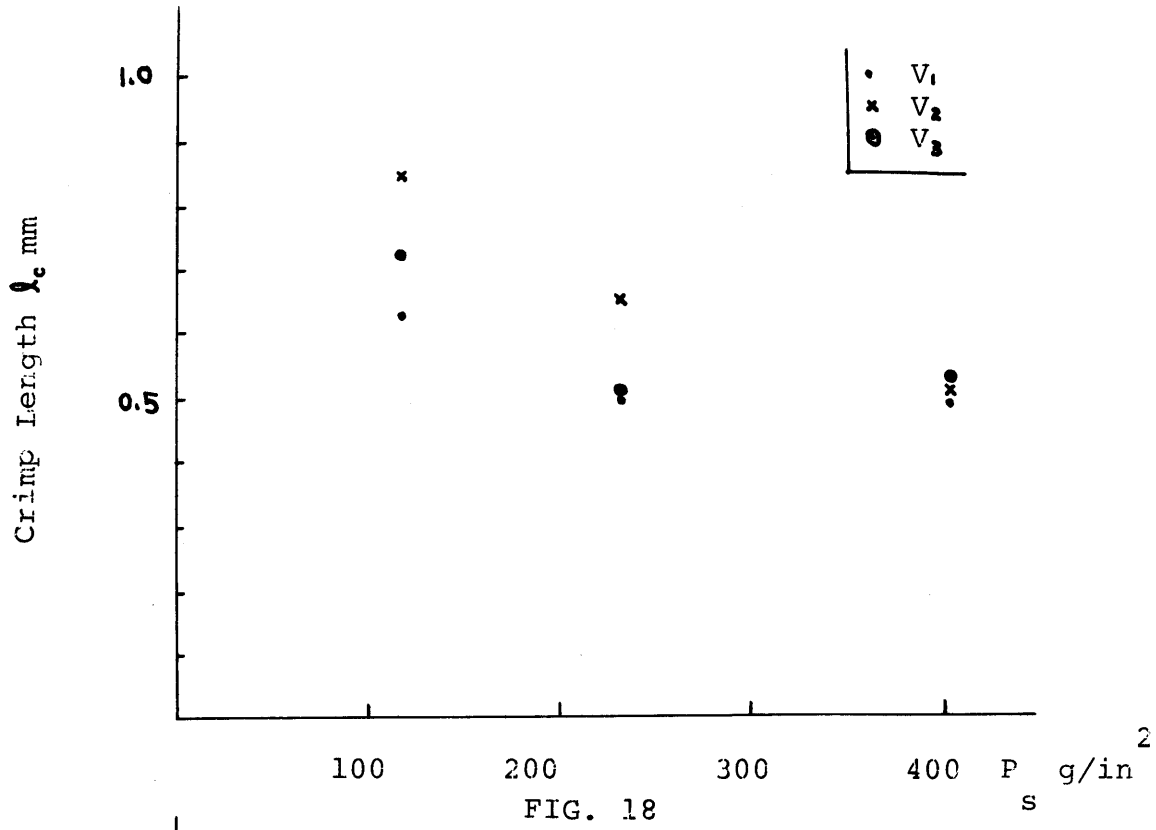
1.0
0.5
Crimp Length ℓ_c mm
V_1
V_2
V_3
100
200
300
400
P_s g/in^2

FIG. 18

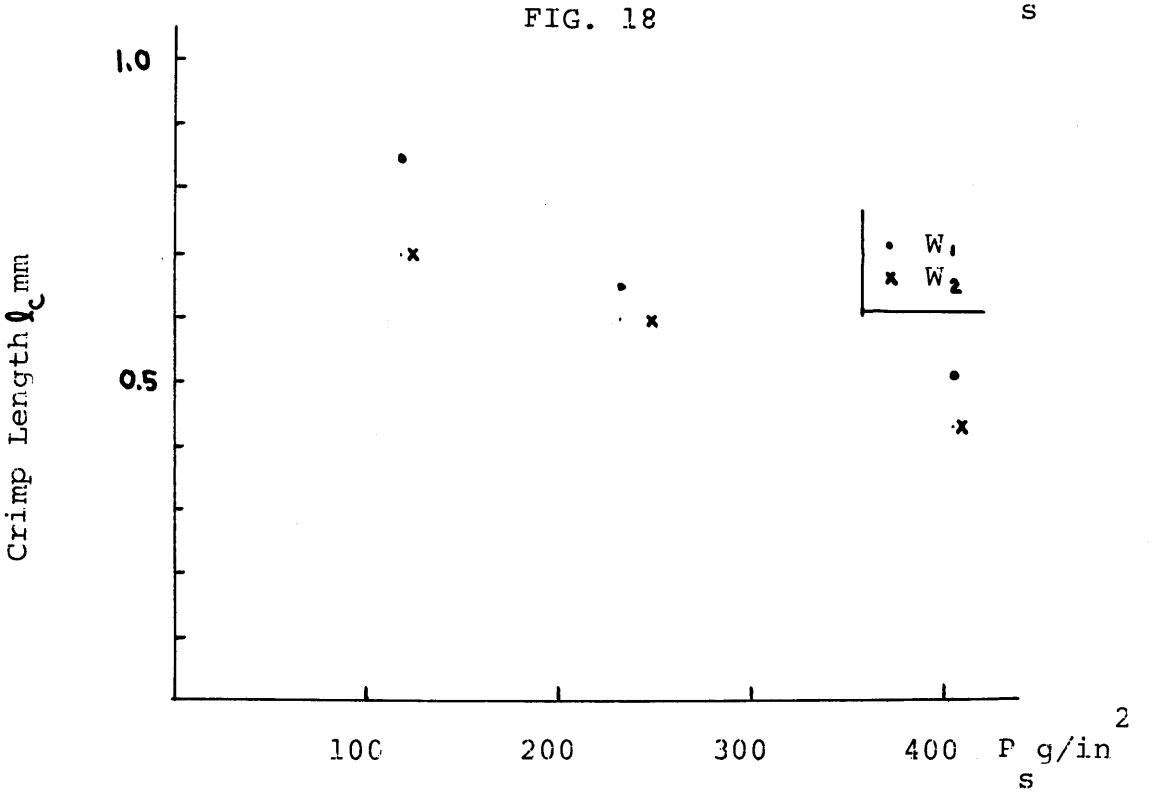
1.0
0.5
Crimp Length ℓ_c mm
W_1
W_2
100
200
300
400
P_s g/in^2

FIG.19

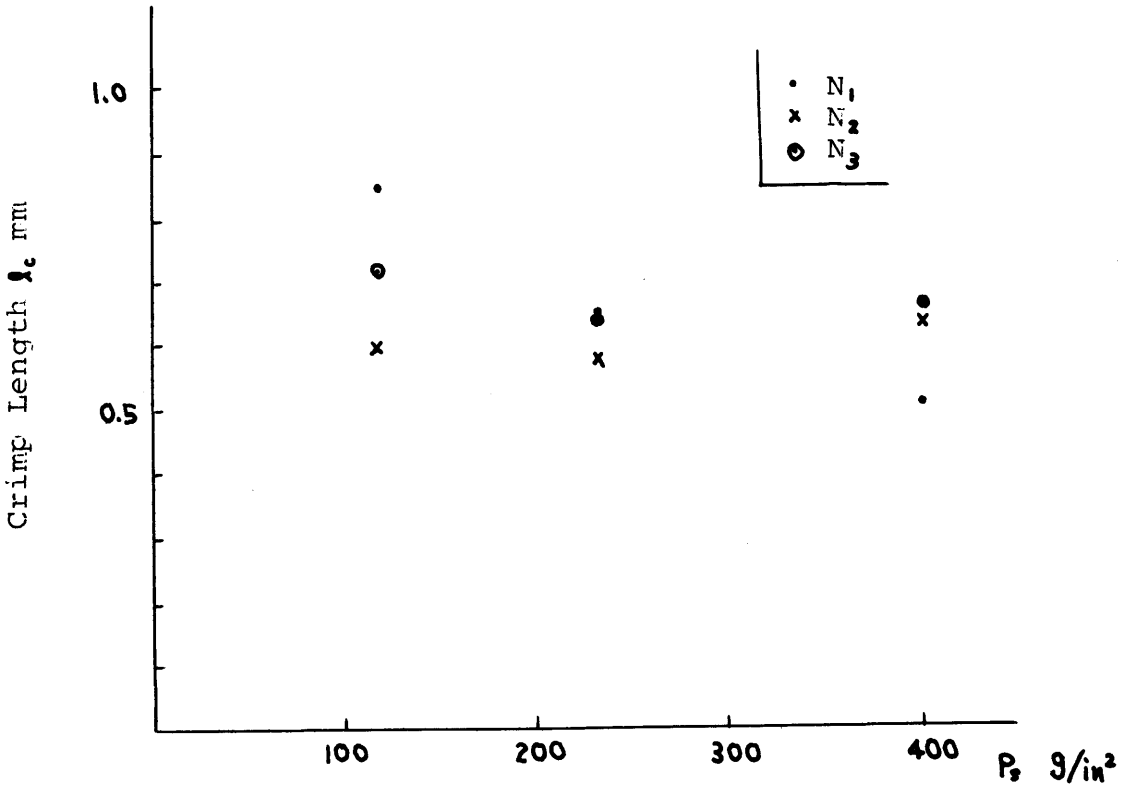
Crimp Length l_c mm
1.0
0.5
N_1
N_2
N_3
100
200
300
400
P_s g/in²

FIG.20

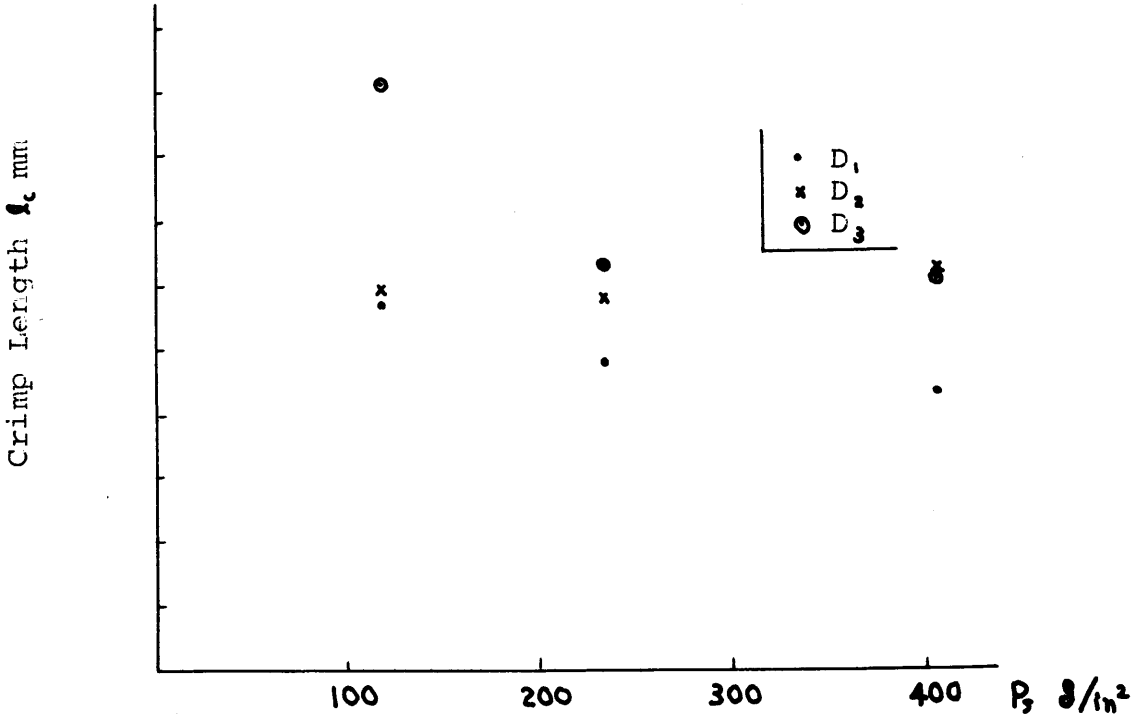
Crimp Length l_c mm
D_1
D_2
D_3
100
200
300
400
P_s g/in²

FIG.21

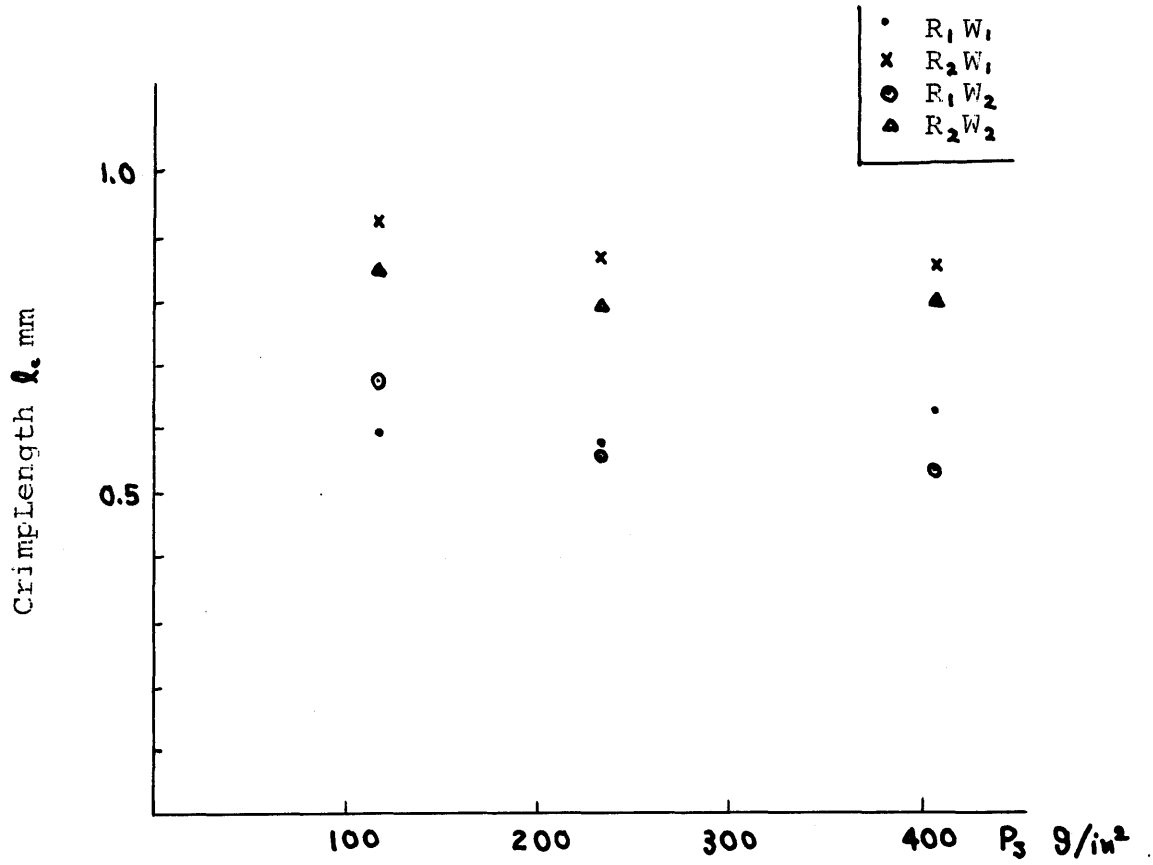
R1 W1
R2 W1
R1 W2
R2 W2
1.0
0.5
Crimp Length ℓc mm
100
200
300
400
Ps g/in²

FIG.22

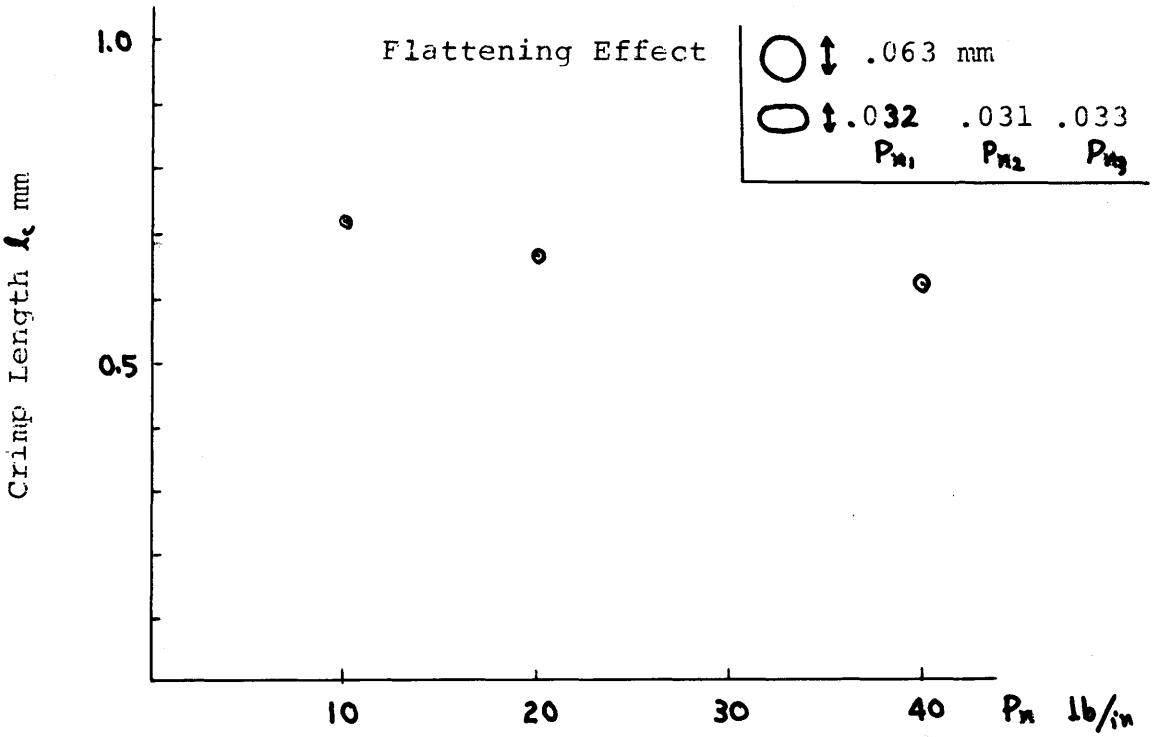
Flattening Effect
.063 mm
.032
.031
.033
1.0
0.5
Crimp Length ℓc mm
10
20
30
40
lb/in

FIG. 23

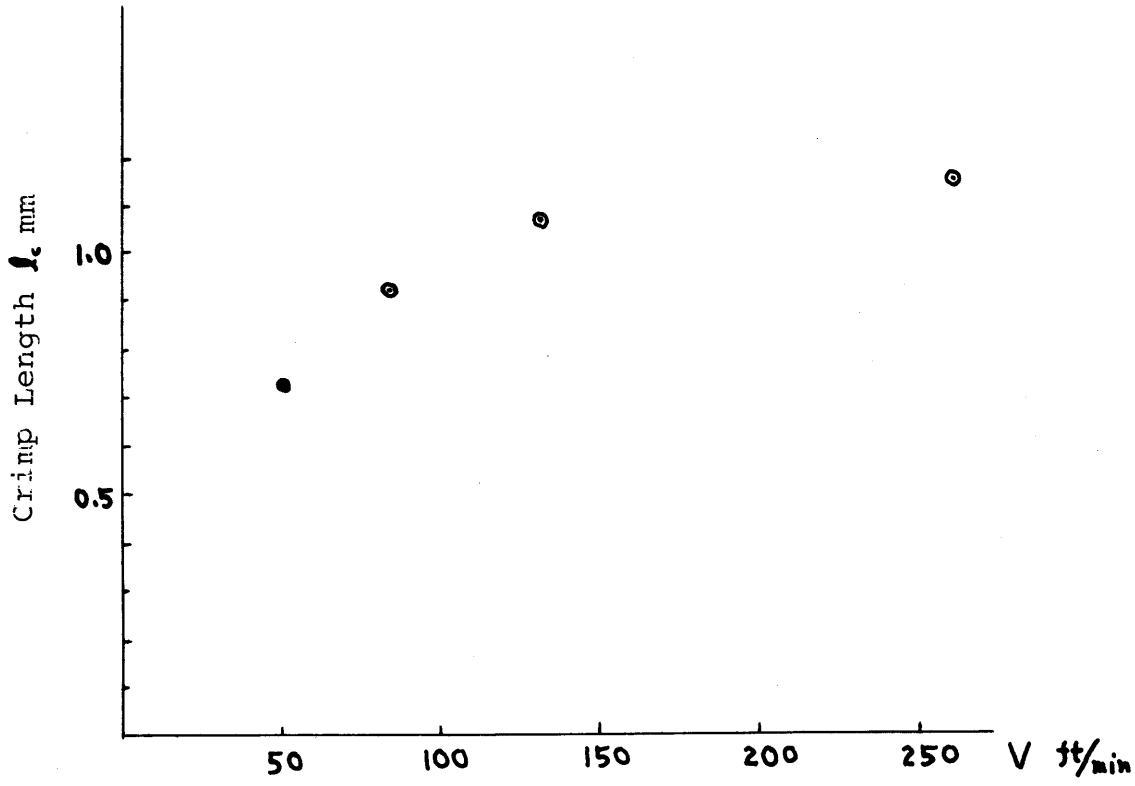
Crimp Length l_c mm
1.0
0.5
50
100
150
200
250
V ft/min

FIG.24

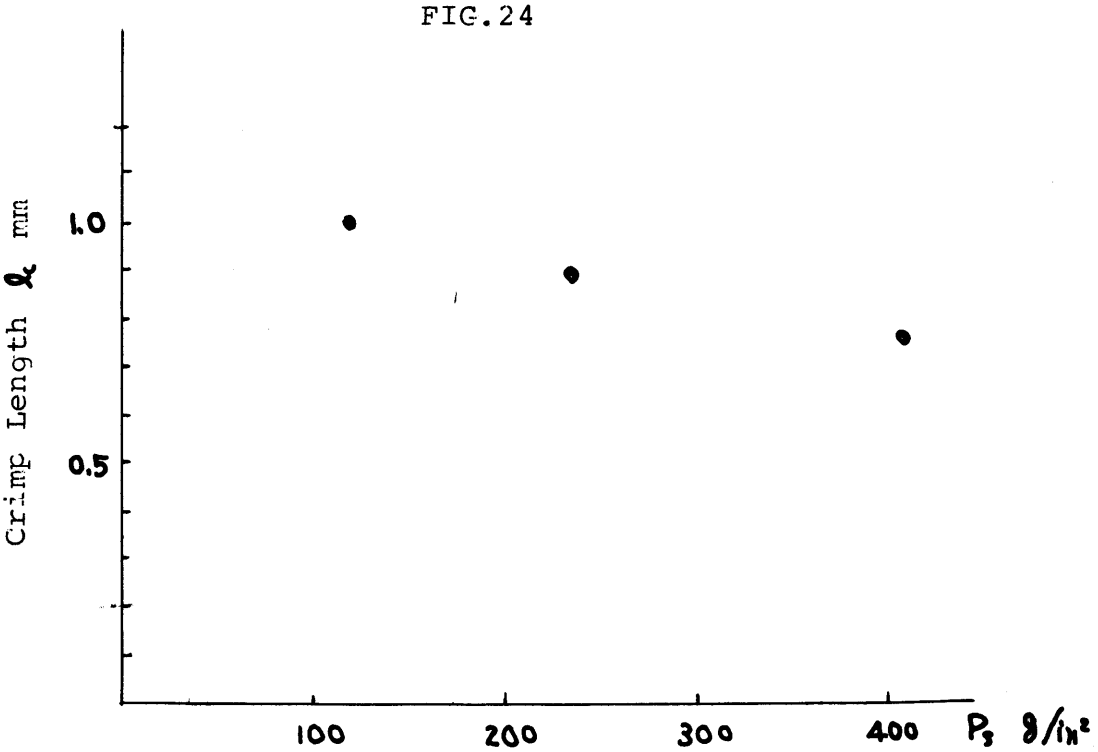
Crimp Length l_c mm
1.0
0.5
100
200
300
400
P_s g/in²

FIG.25

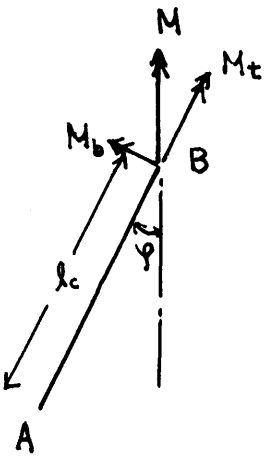

FIG. 50 Isolated Unit for Bending Consideration

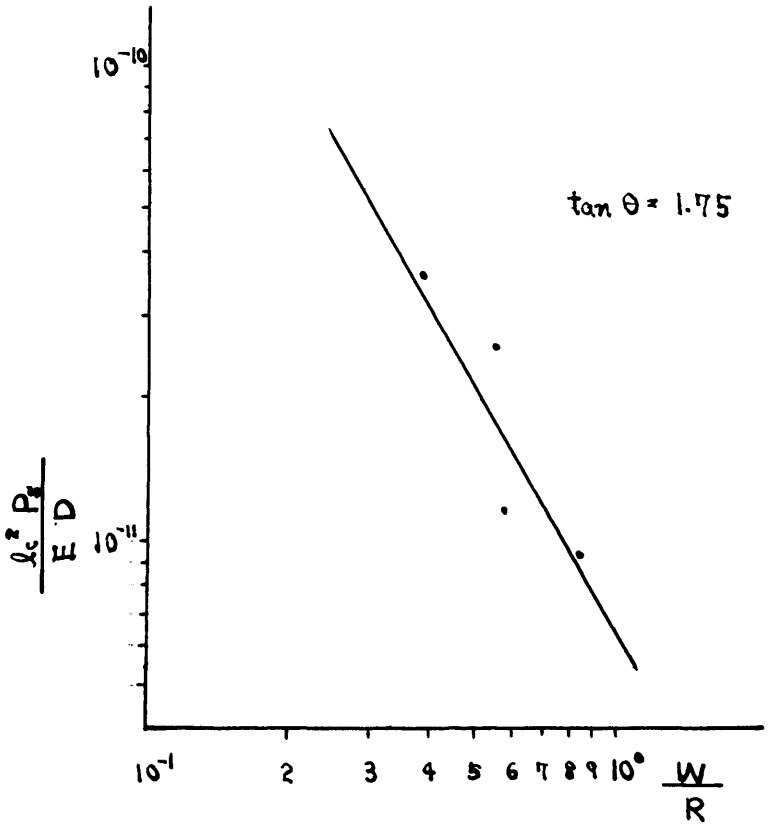

FIG. 51 Effect of W/R (Dimensional Analysis)

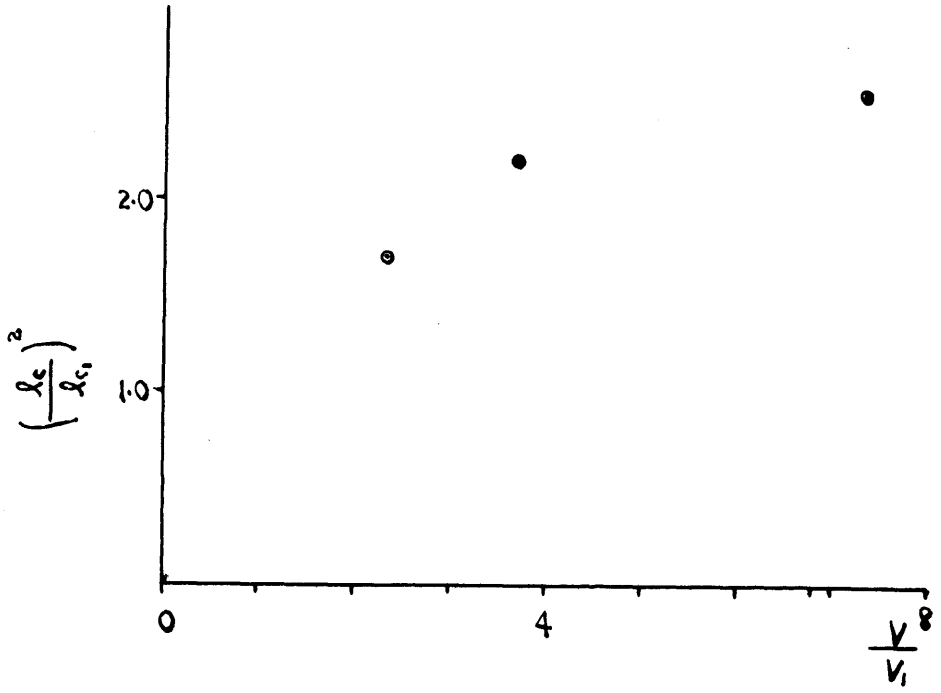

FIG. 52 Effect of V/V$_1$ (Dimensional Analysis)